

~~R700243~~

AD 202 126

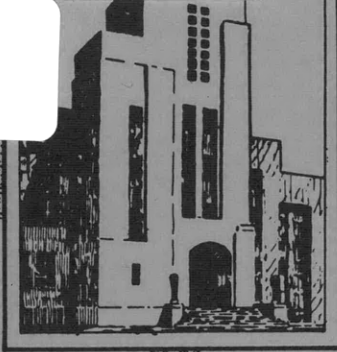
Report 1024

MIT LIBRARIES



3 9080 02754 2171

V393  
.R46



NAVY DEPARTMENT  
**DAVID TAYLOR MODEL BASIN**

HYDROMECHANICS



AERODYNAMICS



STRUCTURAL  
MECHANICS

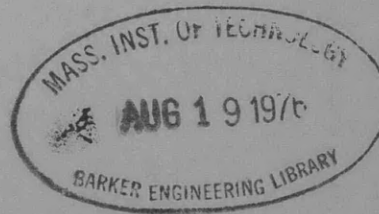


APPLIED  
MATHEMATICS

THE FRICTIONAL RESISTANCE AND TURBULENT BOUNDARY  
LAYER OF ROUGH SURFACES

by

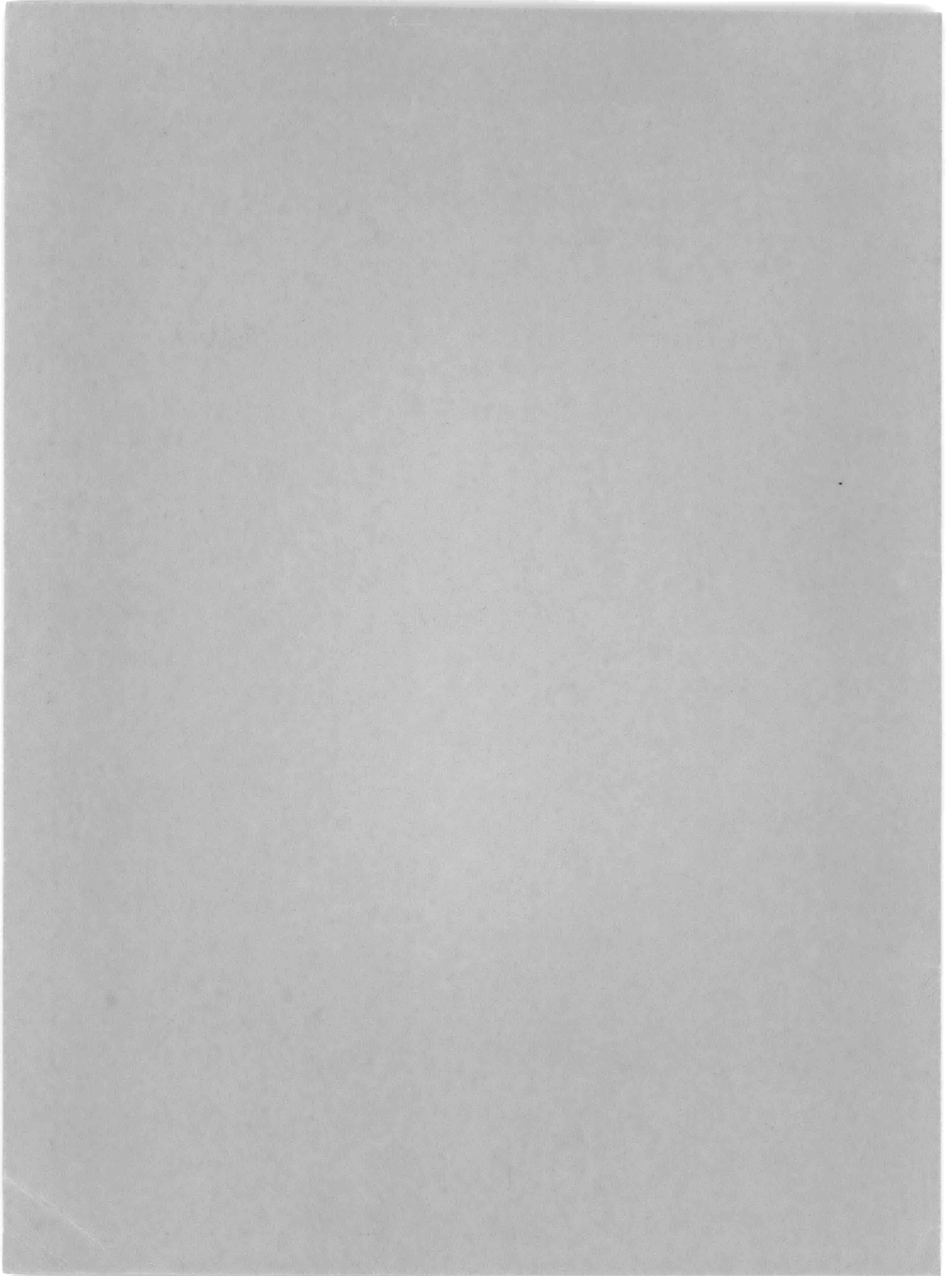
Paul S. Granville



HYDROMECHANICS LABORATORY  
RESEARCH AND DEVELOPMENT REPORT

June 1958

Report 1024



**THE FRICTIONAL RESISTANCE AND TURBULENT BOUNDARY  
LAYER OF ROUGH SURFACES**

**by**

**Paul S. Granville**

**June 1958**

**Report 1024**

## TABLE OF CONTENTS

	Page
ABSTRACT.....	1
INTRODUCTION .....	1
<b>BOUNDARY-LAYER CHARACTERISTICS FROM SIMILARITY LAWS .....</b>	<b>3</b>
General .....	3
Inner Law or Law of the Wall .....	3
Outer Law or Velocity-Defect Law .....	4
Logarithmic Velocity Law .....	4
Types of Flow Regimes on Rough Surfaces .....	6
Sublayers within Turbulent Shear Flows .....	7
Velocity Law for the Laminar Sublayer .....	9
Velocity Law for the Transitional Sublayer of Smooth Surfaces .....	9
Velocity Law for the Transitional Sublayer of the General Rough Regime .....	13
Velocity Law for the Transitional Sublayer of the Fully Rough Regime .....	14
Boundary-Layer Parameters .....	17
<b>FRICITIONAL RESISTANCE OF FLAT PLATES .....</b>	<b>20</b>
General .....	20
Fully Rough Regime .....	24
Quasi-Smooth Regime .....	25
Engineering Roughness .....	26
<b>APPLICATION OF THE GENERAL LOGARITHMIC RESISTANCE FORMULA TO ARBITRARY ROUGHNESS .....</b>	<b>28</b>
Preparation of Resistance Diagrams from Resistance Characterizations .....	28
Resistance Characterizations from Plate Tests .....	30
Prediction of Full-Scale Resistance from Plate Tests .....	33
<b>LOCAL SKIN FRICTION COEFFICIENTS AND SHAPE PARAMETERS .....</b>	<b>35</b>
General .....	35
Fully Rough Regime .....	36
Quasi-Smooth Regime .....	37
Engineering Roughness .....	38
Preparation of Local Skin Friction Coefficient and Shape Parameter Diagrams from Resistance Characterizations .....	39
Preparation of Local Skin Friction Coefficient and Shape Parameter Diagrams from Plate Tests .....	40

	Page
NUMERICAL RESULTS .....	41
ACKNOWLEDGMENT .....	44
REFERENCES.....	44

### LIST OF ILLUSTRATIONS

Figure 1 – Resistance Characterization for Roughness in Pipes.....	7
Figure 2 – Sublayers within Turbulent Shear Flows .....	8
Figure 3 – Comparison of Various Formulations for Transitional Sublayer of Smooth Pipes.....	12
Figure 4 – Variation of Transitional Sublayer Factors for Nikuradse Sand Rough Pipes .....	14
Figure 5 – Plot of Inner Law for Nikuradse’s Sand Rough Pipe Data .....	16
Figure 6 – Plot of Inner Law for Nikuradse’s Sand Rough Pipe Data .....	16
Figure 7 – Resistance Diagram for Rough Plates with Sand Roughness and Engineering Roughness .....	31
Figure 8 – Resistance Characterization of Roughness from Flat Plate Resistance Data.....	32
Figure 9 – Resistance Prediction Diagram for Rough Plates .....	34
Figure 10 – Values of $B_2$ for Sand Roughness in Pipes and on Flat Plates .....	42
Figure 11 – Coefficients of Total Resistance for the Fully Rough Regime .....	43
Figure 12 – Local Skin Friction and Shape Parameter for the Fully Rough Regime of Flat Plates .....	43

### LIST OF TABLES

Table 1 – Summary of Factors for the Velocity Laws of Transitional Sublayers .....	17
Table 2 – Velocity Profile Integrals .....	18
Table 3 – Numerical Values of Factors .....	41

## NOTATION

$A$	Slope of logarithmic velocity law
$a_1, a_2, a_3, a_4$	Linearization constants
$B_1, B_2, B_3$	Intercepts of logarithmic velocity law; see Equations [7], [8], and [10]
$B_{1,s}$	$B_1$ for smooth surfaces
$B_{2,R}$	$B_2$ for fully rough regime
$B_2'$	Derivative of $B_2$ with respect to $\ln k^*$ , Equation [76]
$B_2''$	Derivative of $B_2'$ with respect to $\ln k^*$ , Equation [77]
$C_f$	Coefficient of total resistance; see Equation [67]
$C_\tau$	Coefficient of local resistance; see Equation [13]
$C_1, C_2, C_3, C_4$	Linearization constants; see Equations [91] and [95]
$D_1, D_2$	Velocity profile constants; see Table 2
$e$	Base of natural logarithms
$F$	Outer law function, Equation [4]
$f_1, f_2$	Inner law functions, Equations [2] and [3]
$G$	Subscript for quantities at junction of inner and outer turbulent sublayers; see Table 2
$H$	Shape parameter, Equation [63]
$I_1, I_2$	Integrals of outer law velocity profiles; see Table 2
$J_1, J_2$	Transitional sublayer factors, Equations [42] and [44]
$k, k_1, k_2, \dots$	Linear parameters defining roughness
$k^*$	Roughness Reynolds number; see Equation [2]
$k_R^*$	Value of $k^*$ at start of fully rough regime, Equation [53]
$k_s^*$	Value of $k^*$ at end of quasi-smooth regime
$L$	Subscript for quantities at junction of laminar and transitional sublayers; see Table 2
$l$	Mixing length
$M_1, M_2$	Constants in logarithmic resistance formulas for flat plates, Equations [93] and [98]
$m$	Constant in logarithmic resistance formula for flat plates with engineering roughness, Equation [117]

$N_1, N_1', N_2$	Constants in logarithmic resistance formulas for flat plates, Equations [94], [99] and [103]
$O_1, O_2$	Constants in local resistance formulas, Equations [145] and [150]
$P_1, P_1', P_2$	Constants in local resistance formulas, Equations [146], [156] and [151]
$R_f$	Frictional resistance
$R_x$	Reynolds number based on length
$R_\theta$	Reynolds number based on momentum thickness, Equation [61]
$r$	Factor given in Equation [172]
$s$	Subscript representing smooth conditions
$T$	Subscript for quantities at junction of transitional and inner turbulent sublayers; see Table 2
$U$	Velocity at outer edge of boundary layer
$u$	Tangential velocity in boundary layer
$u'$	Fluctuation in $u$
$u_\tau$	Shear velocity
$v'$	Fluctuation in normal velocity
$x$	Distance along boundary layer
$x^*$	Nondimensional $x$ , Equation [124]
$y$	Normal distance from wall
$y^*$	Nondimensional $y$
$\alpha_1, \alpha_2$	Velocity profile constants; see Table 2
$\beta_1, \beta_2$	Velocity profile constants; see Table 2
$\gamma$	Constant in logarithmic resistance formula for flat plates with engineering roughness, Equation [116]
$\delta$	Boundary layer thickness
$\delta^*$	Displacement thickness
$\epsilon$	Boussinesq eddy viscosity, Equation [22]
$\theta$	Momentum thickness
$\kappa$	Slope of $\epsilon$ with respect to $y$
$\lambda$	Constant for engineering roughness, Equation [109]

$\mu$	Viscosity of fluid
$\nu$	Kinematic viscosity, $\mu/\rho$
$\rho$	Density of fluid
$\sigma$	Local resistance parameter, $U/u_\tau$
$\tau$	Shearing stress
$\tau_w$	Shearing stress at wall



## ABSTRACT

By means of the similarity laws of the turbulent flow in boundary layers, a general relation is developed for the frictional resistance of flat plates with arbitrary roughness from which logarithmic formulas are obtained for the special cases of the fully rough regime, the quasi-smooth regime, and engineering roughness. Among other uses, this general relation permits for the first time a simple rational extrapolation to full-scale conditions of the frictional resistance of model plates covered uniformly with any irregular full-scale roughness encountered in practice. Furthermore, for calculations of turbulent boundary layers in pressure gradients on rough surfaces, relations are derived for the local skin friction and velocity profile shape parameter in terms of momentum thickness Reynolds number. Simplified relations are also derived for the velocity profile of the transitional sublayer in the vicinity of a rough surface.

## INTRODUCTION

The analysis and prediction of the frictional resistance or drag of rough surfaces presents in general a more complex problem than that of smooth surfaces owing to the geometric diversity of roughness and the accompanying involved effect on turbulent flow.

Since research into the fundamentals of turbulence has yet to achieve a method for predicting frictional resistance, recourse as in the case of smooth surfaces is made to the similarity characteristics of the mean-velocity profiles of shear flows for a general method of analyzing the resistance of rough surfaces.

For turbulent shear flows, such as fully developed viscous flow in pipes or boundary-layer flow on flat plates, the two laws which provide similarity in the mean-velocity profile by linking it to the wall shearing stress are:

1. The inner law or law of the wall which applies to the flow immediately adjacent to the solid boundary.
2. The outer law or velocity-defect law which applies to the remaining outer region of the shear flow.

The overlapping of the range of application of the two laws requires a logarithmic functional form for both similarity laws within the common region of overlap.

The similarity laws of the velocity profile were originally developed for pipe flows by Prandtl<sup>1</sup> and separately by Von Kármán,<sup>2, 3</sup> though with some significant differences. Prandtl

---

<sup>1</sup>References are listed on page 44.

used the logarithmic form for the velocity profile of the whole flow which in effect assumed the region of overlap of the two similarity laws to extend over the whole flow. Von Kármán, on the other hand in a more general presentation, used the logarithmic form for only a limited region of overlap and wrote the outer law as an unspecified functional relation for the flow outside the region of overlap. The difference between the Prandtl and Von Kármán procedures is not significant for pipe flows since a logarithmic form fits very closely most of the flow, but it is significant for boundary-layer flows on flat plates since a logarithmic form fits adequately only about 15 percent of the flow.

Inasmuch as the differences between pipe and flat-plate flows were not apparent at the time, Prandtl and Schlichting<sup>4</sup> used the simpler Prandtl procedure of a logarithmic form for the whole boundary-layer flow as well as numerical values from pipe tests in determining the resistance of rough plates from Nikuradse's<sup>5</sup> tests on pipes coated with sand grains. Consequently, one of the purposes of this report is to determine the resistance of sand-coated plates by applying Von Kármán's procedure of a limited logarithmic region together with the somewhat different numerical values from flat-plate tests.

More importantly, the whole subject of the application of the similarity laws to the resistance of rough plates is developed in detail. The logarithmic form of the similarity laws in the region of overlap is derived in a simple fashion which emphasizes the nature of the resulting constants. Detailed consideration is given to delineating the different sublayers within the boundary layer. Expressions are derived for the velocity profile of transitional sublayers of rough surfaces by an extension of a method of Squire<sup>6</sup> for smooth surfaces. The boundary-layer factors of displacement thickness, momentum thickness, and shape parameter are determined for rough surfaces by combining integrated quantities of the velocity profiles of the separate sublayers.

The relation for momentum thickness is then used to determine the coefficient of total resistance of flat plates as a function of Reynolds number and relative roughness in terms of a local-resistance parameter for the general case of roughness. Then by eliminating the local-resistance parameter and dropping terms which become negligible at larger boundary-layer thicknesses, a simpler logarithmic formula is obtained for the total resistance coefficient of flat plates with arbitrary roughness. From this, special logarithmic resistance formulas are developed for the special cases of the fully rough regime, the quasi-smooth regime, and engineering roughness.

The general logarithmic resistance formula is used to prepare resistance charts from empirical roughness characterizations, to obtain roughness characterizations from total resistance data, and to predict full-scale resistance from plate tests with arbitrary roughness. The last procedure should be especially useful in studying the frictional resistance of ship hulls in newly painted and in fouled conditions. Towing a representative sample of the hull roughness would be required instead of difficult full-scale trials.

Finally relations are derived for the local skin friction and the velocity profile shape parameter for use in calculations of turbulent boundary layers in pressure gradients. A method of obtaining such information from towing tests of plates with arbitrary roughness is also included.

## BOUNDARY-LAYER CHARACTERISTICS FROM SIMILARITY LAWS

### GENERAL

First, an important distinction should be emphasized between the similarity laws and their historical association with turbulence hypotheses, like the mixing-length theory, which have become somewhat untenable by reason of more detailed experimental investigations<sup>7, 8</sup> into the nature of energy transfer in shear flow. As statements of general functional relationships, the similarity laws can have their basis in purely dimensional arguments supported by experimental data and thus be made independent of the mixing-length and like theories.

In the past it was mainly for the purpose of deriving specific functional relations that hypotheses concerning the turbulence mechanism had been introduced into the analysis. These were the mixing-length theory and assumptions about the laminar sublayer by Prandtl<sup>1</sup> in obtaining the logarithmic form of the inner law, and a similarity hypothesis of the turbulent flow pattern by Von Kármán<sup>3</sup> in formulating his particular expression for the outer law. All this can be avoided since the logarithmic form can be derived from the overlapping of the inner and outer laws and the outer law elsewhere can be analytically treated as an unspecified function in arriving at the desired resistance formulas.

### INNER LAW OR LAW OF THE WALL

Close to the wall or solid boundary the distribution of the mean velocity  $u$  of the turbulent flow parallel to the wall is considered to depend on the normal distance  $y$  away from the wall, the shearing stress  $\tau_w$  at the wall, the density  $\rho$  and viscosity  $\mu$  of the fluid, and various linear parameters defining the roughness of the wall  $k, k_1, k_2, \dots$ , or

$$u = f(y, \tau_w, \rho, \mu, k, k_1, k_2, \dots) \quad [1]$$

There is in addition the boundary condition at the wall,  $u = 0$  at  $y = 0$ , to be satisfied. By dimensional analysis the variables can be grouped significantly into the following nondimensional ratios:

$$\frac{u}{u_\tau} = f_1 \left( y^*, k^*, \frac{k}{k_1}, \frac{k_1}{k_2}, \dots \right) \quad [2]$$

or

$$\frac{u}{u_\tau} = f_2 \left( \frac{y}{k}, k^*, \frac{k}{k_1}, \frac{k_1}{k_2}, \dots \right) \quad [3]$$

where  $u_\tau = \sqrt{\frac{\tau_w}{\rho}}$  is a factor having the dimensions of velocity and hence called the friction or shear velocity,  $\nu = \frac{\mu}{\rho}$  is the kinematic viscosity of the fluid,  $y^* = \frac{u_\tau y}{\nu}$ , and  $k^* = \frac{u_\tau k}{\nu}$ .

Empirically, Equation [2] or [3] which is the statement of the inner law is uniquely defined for fully developed turbulent flow in pipes regardless of the pipe diameter Reynolds number. A similar but somewhat different numerical relationship holds uniquely for flat plates independent of plate length Reynolds number. In addition the inner law has been found to be independent of pressure gradients.<sup>9</sup>

## OUTER LAW OR VELOCITY-DEFECT LAW

For the turbulent stream at some distance away from the wall the velocity-defect ratio

$\frac{U-u}{u_\tau}$ , where  $U$  is the maximum velocity, is found experimentally to be directly independent of

viscosity and a function only of its relative position in the flow or

$$\frac{U-u}{u_\tau} = F\left(\frac{y}{\delta}\right) \quad [4]$$

where  $\delta$  is the thickness of the shear flow. The boundary condition  $u = U$  at  $y = \delta$  is to be also satisfied. The function  $F$  has been found empirically to be independent of Reynolds number and, most significantly, of the roughness of the wall.<sup>3</sup>

The function  $F$  is numerically different for boundary-layers on flat plates than for pipe flow owing mainly to the presence of the free outer boundary of boundary-layer flow which has been found to have undulating characteristics.<sup>9</sup> It is also markedly affected by longitudinal pressure gradients.<sup>10</sup>

## LOGARITHMIC VELOCITY LAW

Within the boundary layer there is a region where both the inner and outer laws are considered valid. This overlapping leads to a logarithmic relation which will now be derived by a simplified version of Millikan's<sup>11</sup> original demonstration.

Equating the derivative of velocity  $u$  with respect to distance  $y$  of the inner and outer laws, Equations [2] and [4], results in

$$\frac{\partial u}{\partial y} = \frac{u_\tau^2}{\nu} \frac{\partial f_1}{\partial y^*} = - \frac{u_\tau}{\delta} \frac{dF}{d(y/\delta)} \quad [5]$$

or

$$y^* \frac{\partial f_1}{\partial y^*} = - \left( \frac{y}{\delta} \right) \frac{dF}{d(y/\delta)} = A \quad [6]$$

Since the left-hand side of Equation [6] is only a function of  $y^*$  and roughness parameters  $k^*, \frac{k}{k_1}, \frac{k_1}{k_2}, \dots$  and the right-hand side is only a function of  $\frac{y}{\delta}$ , the only quantity satisfying

these conditions is a constant  $A$  independent of all these variables.

From the left-hand side there results after integration

$$f_1 = \frac{u}{u_\tau} = A \ln y^* + B_1 \left( k^*, \frac{k}{k_1}, \frac{k_1}{k_2}, \dots \right) \quad [7]$$

where the constant of integration  $B_1$  is necessarily a function of  $k^*, \frac{k}{k_1}, \frac{k_1}{k_2}, \dots$  from the in-

tegration of a partial derivative. Equation [7] is the statement of the inner law in the region of overlap. An alternate expression is

$$\frac{u}{u_\tau} = A \ln \frac{y}{k} + B_2 \left( k^*, \frac{k}{k_1}, \frac{k_1}{k_2}, \dots \right) \quad [8]$$

where

$$B_2 = B_1 + A \ln k^* \quad [9]$$

From the right-hand side of Equation [6] the outer law in the region of overlap is

$$F = \frac{U-u}{u_\tau} = -A \ln \frac{y}{\delta} + B_3 \quad [10]$$

This establishes the logarithmic form of both the inner and outer laws in the region of overlap. A very important result is that the factor  $B_1$  or  $B_2$  is seen to be solely a function

of roughness Reynolds number  $k^*$  for a particular roughness configuration,  $\frac{k}{k_1}, \frac{k_1}{k_2}, \dots$ ,

and that  $A$  is independent of roughness. Hence the frictional effects of any particular roughness may be considered defined when  $B_1$  or  $B_2$  is experimentally determined as a function of  $k^*$ . This will be termed the *resistance characterization* of a roughness configuration.

Now equating the velocities from the inner and outer laws in the region of overlap gives important relations for the local skin friction.

From Equations [7] and [10]

$$\sigma \equiv \frac{U}{u_{\tau}} = A \ln \frac{u_{\tau} \delta}{\nu} + B_3 + B_1 \quad [11]$$

or from Equations [8] and [10]

$$\sigma \equiv \frac{U}{u_{\tau}} = A \ln \frac{\delta}{k} + B_3 + B_2 \quad [12]$$

where  $\sigma$  is a local resistance parameter. With local coefficient of resistance

$$C_{\tau} \equiv \frac{2\tau_w}{\rho U^2} = 2 \left( \frac{u_{\tau}}{U} \right)^2 = \frac{2}{\sigma^2} \text{ the preceding equations appear as}$$

$$\frac{\sqrt{2}}{\sqrt{C_{\tau}}} = A \ln \left[ \sqrt{C_{\tau}} \left( \frac{U\delta}{\nu} \right) \right] + B_3 + B_1 \quad [13]$$

or

$$\frac{\sqrt{2}}{\sqrt{C_{\tau}}} = A \ln \frac{\delta}{k} + B_3 + B_2 \quad [14]$$

## TYPES OF FLOW REGIMES ON ROUGH SURFACES

In Figure 1, which shows the resistance characterization for Nikuradse's sand rough pipes, it is seen that  $B_1$  is constant for small values of  $k^*$  and that  $B_2$  is constant for large values of  $k^*$ . For intermediate values of  $k^*$ , both  $B_1$  and  $B_2$  vary with  $k^*$ . From this the following classification of turbulent flow past rough surfaces can be made which is significant from the viewpoint of skin friction:

### 1. Quasi-smooth regime

For small values of  $k^*$  starting from zero,  $B_1$  is constant with respect to  $k^*$  and has the same value as for a smooth flow. According to Equation [9],  $B_2$  then plots as a straight line. Most important of all as given by Equation [13] the local coefficient of resistance  $C_{\tau}$  is the same as for a smooth surface and is solely a function of Reynolds number  $\frac{U\delta}{\nu}$ .

### 2. General rough regime

With  $B_1$  and  $B_2$  both varying with  $k^*$ ,  $C_{\tau}$  is a function of Reynolds number  $\frac{U\delta}{\nu}$  and relative roughness  $\frac{k}{\delta}$ .

$$\left[ k^* = \sqrt{\frac{C_{\tau}}{2}} \left( \frac{U\delta}{\nu} \right) \left( \frac{k}{\delta} \right) \right].$$

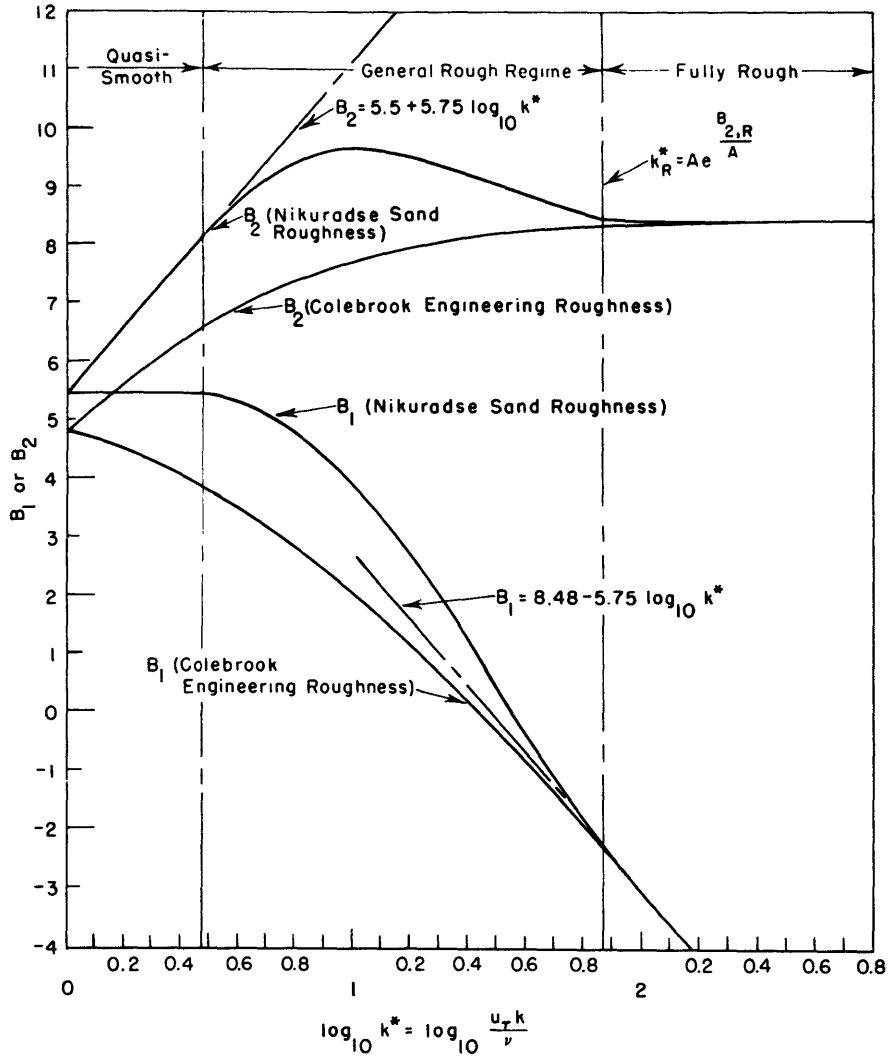


Figure 1 – Resistance Characterization for Roughness in Pipes

### 3. Fully rough regime

At large values of  $k^*$ ,  $B_2$  is constant with respect to  $k^*$  and  $B_1$  plots as a straight line according to Equation [9].  $C_f$  is solely a function of the relative roughness  $\frac{k}{\delta}$  and independent of Reynolds number.

## SUBLAYERS WITHIN TURBULENT SHEAR FLOWS

Various sublayers within the turbulent shear flow can be distinguished according to the behavior of the velocity profiles as indicated schematically in Figure 2. From the wall outward the sublayers are in succession:

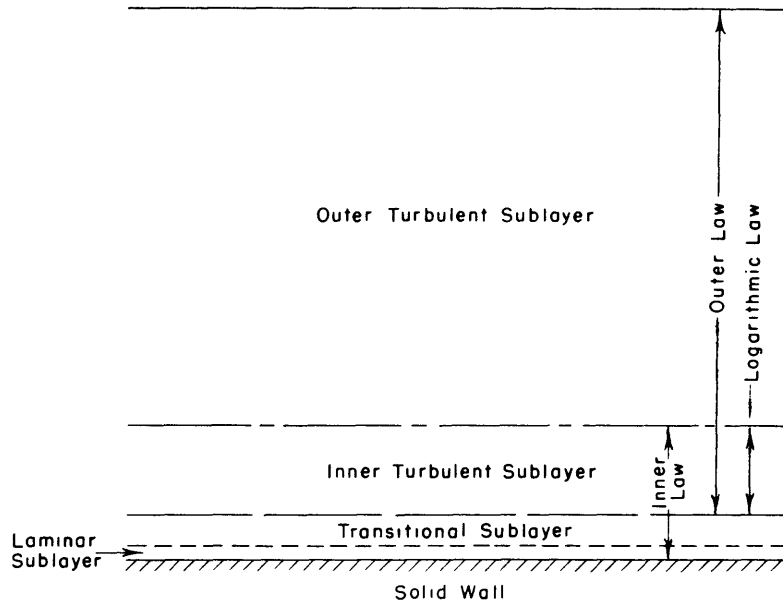


Figure 2 – Sublayers within Turbulent Shear Flows

1. Laminar sublayer

This is the very thin layer in contact with the wall where the flow is laminar and consequently the shearing stress  $\tau$  is given by

$$\tau = \mu \frac{du}{dy} \quad [15]$$

The thickness of the laminar sublayer diminishes with increasing roughness, and finally vanishes in the case of the fully rough flow regime.

2. Transitional sublayer

In this layer the effect of turbulence appears so that the shearing stress is given by

$$\tau = \mu \frac{du}{dy} - \rho \overline{u'v'} \quad [16]$$

where  $-\rho \overline{u'v'}$  is the Reynolds turbulent shearing stress.

3. Inner turbulent sublayer

The inner and outer laws overlap in this layer resulting in the logarithmic velocity law.

4. Outer turbulent sublayer

In this region the wall has no direct effect and the velocity law is the nonlogarithmic part of the outer law.



## VELOCITY LAW FOR THE LAMINAR SUBLAYER

Inasmuch as the inner law Equation [2] provides only the general statement that the velocity ratio  $\frac{u}{u_\tau}$  is a function of Reynolds number  $y^*$  (laminar flow is independent of roughness), other considerations must be applied in order to obtain a specific functional relationship for the laminar sublayer. If the laminar motion within the sublayer is assumed essentially a parallel flow, the shearing stress  $\tau$  is given as

$$\tau = \mu \frac{du}{dy} \quad [17]$$

Within the thin sublayer the variation of  $\tau$  with  $y$  is negligible; hence

$$\tau = \tau_w \quad [18]$$

Consequently

$$\frac{du}{dy} = \frac{\tau_w}{\mu} \quad [19]$$

and with  $u = 0$  at  $y = 0$ ,

$$u = \frac{\tau_w}{\mu} y \quad [20]$$

or

$$\frac{u}{u_\tau} = y^* \quad [21]$$

Empirical verification for this relation has been obtained by Laufer<sup>7</sup> by measurements in a closed channel.

## VELOCITY LAW FOR THE TRANSITIONAL SUBLAYER OF SMOOTH SURFACES

Expressions for the velocity law of the transitional sublayer for smooth surfaces have been derived by various authors on the basis of assumptions concerning the variation of the turbulent shearing stress with  $y$ . In general, since the shearing stress has both laminar and turbulent contributions,

$$\tau = \mu \frac{du}{dy} - \rho u \overline{v'} \quad [16]$$

where  $-\rho \overline{u'v'}$  is the Reynolds stress formed by the average of the turbulent velocity fluctuations  $u'$  and  $v'$  in the  $x$  and  $y$  directions respectively. If the Boussinesq eddy viscosity  $\epsilon$  is introduced where

$$\epsilon = - \frac{\overline{u'v'}}{\frac{du}{dy}} \quad [22]$$

then

$$\tau = \rho (\nu + \epsilon) \frac{du}{dy} \quad [23]$$

If it is assumed that the variation of  $\tau$  with  $y$  across the thin sublayer is negligible, then  $\tau = \tau_w$  and

$$u_{\tau}^2 = (\nu + \epsilon) \frac{du}{dy} \quad [24]$$

Various investigators have assumed in effect different variations of  $\epsilon$  with  $y$ .

Squire<sup>6</sup> by dimensional reasoning and by considering the turbulence effect to start just at the outer edge of the laminar sublayer uses a linear variation of  $\epsilon$  across the transitional sublayer or

$$\epsilon = \kappa u_{\tau} (y - y_L) \quad [25]$$

where  $\kappa$  is a constant of proportionality and  $y_L$  is the thickness of the laminar sublayer. Other authors use the mixing-length hypothesis wherein

$$\epsilon = l^2 \left| \frac{du}{dy} \right| \quad [26]$$

$l$  being the mixing length. Rotta<sup>12</sup> and Hudimoto<sup>13</sup> independently assume

$$l = \kappa (y - y_L) \quad [27]$$

or

$$\epsilon = \kappa^2 (y - y_L)^2 \left| \frac{du}{dy} \right| \quad [28]$$

Hama<sup>14</sup> uses for both the laminar and transitional sublayers

$$l = \kappa y^2 \quad [29]$$

or

$$\epsilon = \kappa^2 y^4 \left| \frac{du}{dy} \right| \quad [30]$$

whereas Van Driest<sup>15</sup> assumes a still more complicated relation

$$l = \kappa y \left( 1 - e^{-\frac{y}{\text{const}}} \right) \quad [31]$$

or

$$\epsilon = \kappa^2 y^2 \left( 1 - e^{-\frac{y}{\text{const}}} \right)^2 \left| \frac{du}{dy} \right| \quad [32]$$

The procedures of both Squire and Rotta lead to expressions in closed form, that of Squire being much simpler. On the other hand Hama obtained a much more complicated expression involving elliptic integrals and Van Driest obtained a still more unwieldy expression requiring numerical integration. In Figure 3 where the various formulations are compared with Laufer's<sup>16</sup> pipe data, it is to be noted that the simple expression of Squire is an adequate approximation. The method of Squire will be extended in this report to cover the case of rough surfaces. However, full credit is due Rotta<sup>12</sup> for first analyzing the transitional sub-layers of rough surfaces.

Squire's procedure for smooth surfaces will be now completed. Substituting Squire's  $\epsilon$ , Equation [25], into Equation [24] results in

$$\frac{du}{dy} = \frac{u_\tau^2}{\nu + \kappa u_\tau (y - y_L)} \quad [33]$$

Integrating and utilizing the initial condition that

$$\frac{u}{u_\tau} = \frac{u_\tau y_L}{\nu} \text{ at } y = y_L \quad [34]$$

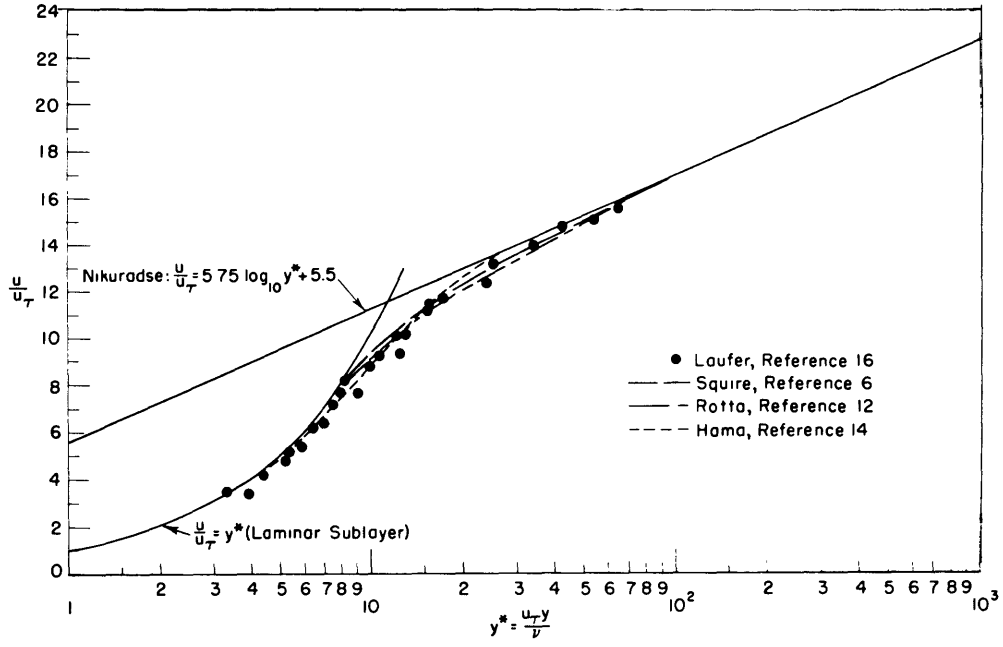


Figure 3 – Comparison of Various Formulations for Transitional Sublayer of Smooth Pipes

yields

$$\frac{u}{u_{\tau}} = \frac{1}{\kappa} \ln \left[ \frac{u_{\tau}(y - y_L)}{\nu} + \frac{1}{\kappa} \right] - \frac{1}{\kappa} \ln \frac{1}{\kappa} + \frac{u_{\tau} y_L}{\nu} \quad [35]$$

or

$$\frac{u}{u_{\tau}} = A \ln \left( y^* - B_1 + A \ln \frac{e}{A} \right) + B_1 \quad [36]$$

where

$$A = \frac{1}{\kappa} \quad [37]$$

$$B_1 = y_L^* - A \ln A \quad [38]$$

or

$$y_L^* = B_1 + A \ln A \quad [39]$$

For large  $y^*$  the velocity law asymptotically becomes

$$\frac{u}{u_\tau} = A \ln y^* + B_1 \quad [40]$$

which is the form for the logarithmic law. Hence the  $A$  and  $B_1$  of Equation [40] and those of the inner law Equation [7] are identical.

It is to be noted that Equation [39] gives the thickness of the laminar sublayer when values for  $B_1$  and  $A$  are substituted in the expression.

### VELOCITY LAW FOR THE TRANSITIONAL SUBLAYER OF THE GENERAL ROUGH REGIME

The velocity law for the smooth transitional sublayer, Equation [36], can be written as

$$\frac{u}{u_\tau} = A \ln (y^* - J_1) + B_1 \quad [41]$$

where

$$J_1 = B_1 - A \ln \frac{e}{A} = y_L^* - A \quad [42]$$

Since  $B_1$  is a function of  $k^*$  for a particular roughness, then  $J_1$  and  $y_L^*$  are also functions of  $k^*$ . For the general rough regime  $J_1$  will have a limiting value of  $-A$  since  $y_L^*$  is zero for the case of the fully rough regime.

The velocity law for the transitional sublayer of the general rough regime may be re-stated as

$$\frac{u}{u_\tau} = A \ln \left( \frac{y}{k} - J_2 \right) + B_2 \quad [43]$$

where

$$J_2 = \frac{y_L^* - A}{k^*} = \frac{J_1}{k^*} = \left( \frac{y}{k} \right)_L - \frac{A}{k^*} \quad [44]$$

Also

$$\left( \frac{y}{k} \right)_L = \frac{B_2 + A \ln \frac{A}{k^*}}{k^*} \quad [45]$$

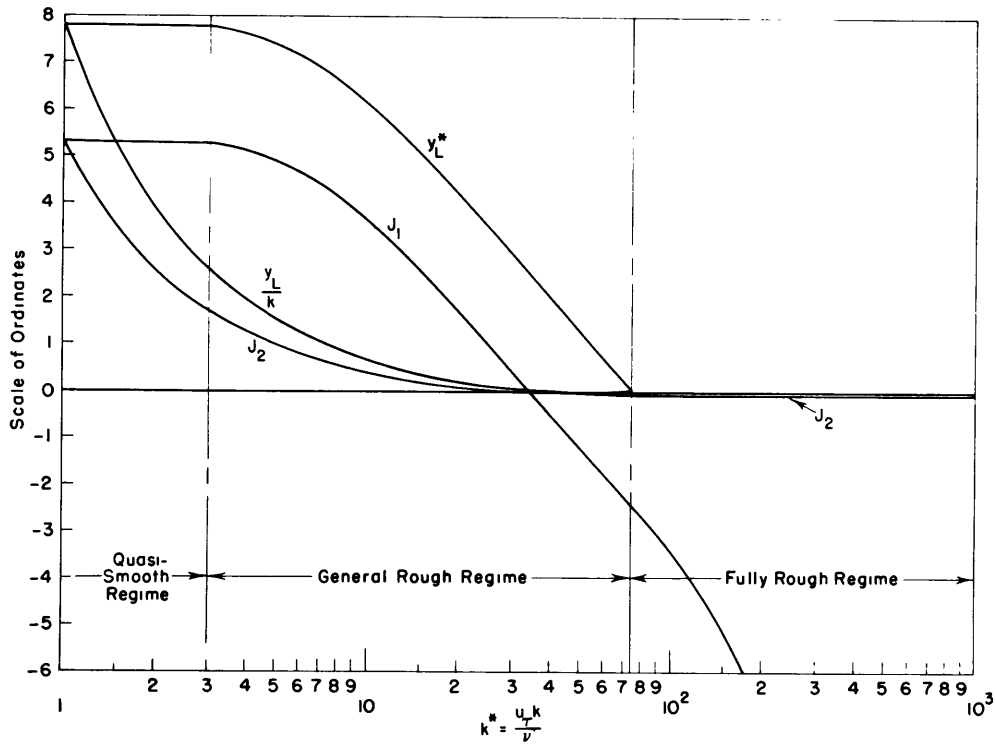


Figure 4 – Variation of Transitional Sublayer Factors for Nikuradse Sand Pough Pipes

Figure 4 shows a plot of  $y_L^*$ ,  $J_1$ , and  $J_2$  as a function of  $k^*$  calculated for Nikuradse's sand rough pipes.

### VELOCITY LAW FOR THE TRANSITIONAL SUBLAYER OF THE FULLY ROUGH REGIME

In this case the laminar sublayer has vanished,  $y_L = 0$ , and the plane of reference for  $y$ ,  $y = 0$ , is defined where the velocity  $u$  is zero on an average over the rough surface. There is then an initial shearing stress due to turbulence represented by  $\epsilon_0$  at the start of the transitional sublayer. Then

$$\epsilon = \epsilon_0 + \kappa u_\tau y \quad [46]$$

and

$$\frac{du}{dy} = \frac{u_\tau^2}{\nu + \epsilon_0 + \kappa u_\tau y} \quad [47]$$

Integrating and utilizing the initial condition  $u = 0$  at  $y = 0$  results in

$$\frac{u}{u_{\tau}} = \frac{1}{\kappa} \ln \left( 1 + \frac{\kappa u_{\tau} y}{\nu + \epsilon_0} \right) \quad [48]$$

or

$$\frac{u}{u_{\tau}} = A \ln \left( \frac{y}{k} - J_2 \right) + B_2 \quad [49]$$

where

$$J_2 = -e^{-\frac{B_2}{A}} \quad [50]$$

and

$$B_2 = A \ln \frac{k^*}{A \left( 1 + \frac{\epsilon_0}{\nu} \right)} \quad [51]$$

It is interesting to observe that when Equation [49] is rewritten as

$$\frac{u}{u_{\tau}} = A \ln \left( e^{\frac{B_2}{A}} \frac{y}{k} + 1 \right) \quad [52]$$

it is identical to the velocity law of Prandtl and Schlichting<sup>4</sup> in which the unit constant had been arbitrarily added to the argument of the logarithm to make  $u/u_{\tau} = 0$  at  $y/k = 0$ . The results for the velocity laws of the transitional sublayer are summarized in Table 1. Representative velocity profiles of the inner law for sand rough pipes are shown in Figures 5 and 6.

Equating Equations [44] and [50] and setting  $y_L^* = 0$  specifies the start of the fully rough regime in terms of

$$k_R^* = A e^{\frac{B_2}{A}} \quad [53]$$

The value of  $k_R^*$  determined from Equation [53] agrees well with the experimental point where  $B_2$  becomes constant as shown in Figure 1.

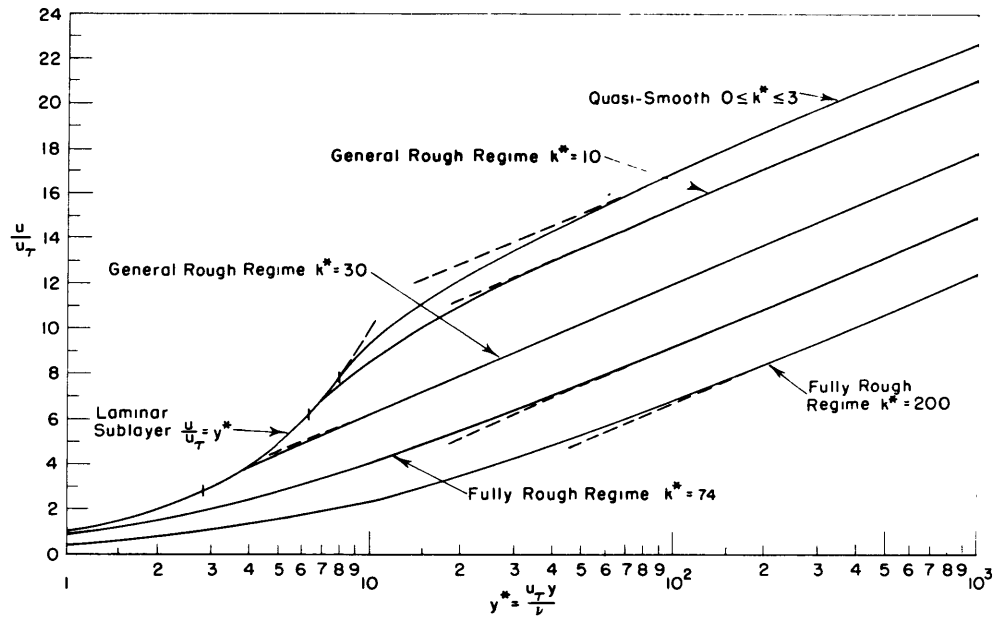


Figure 5 – Plot of Inner Law for Nikuradse's Sand Rough Pipe Data

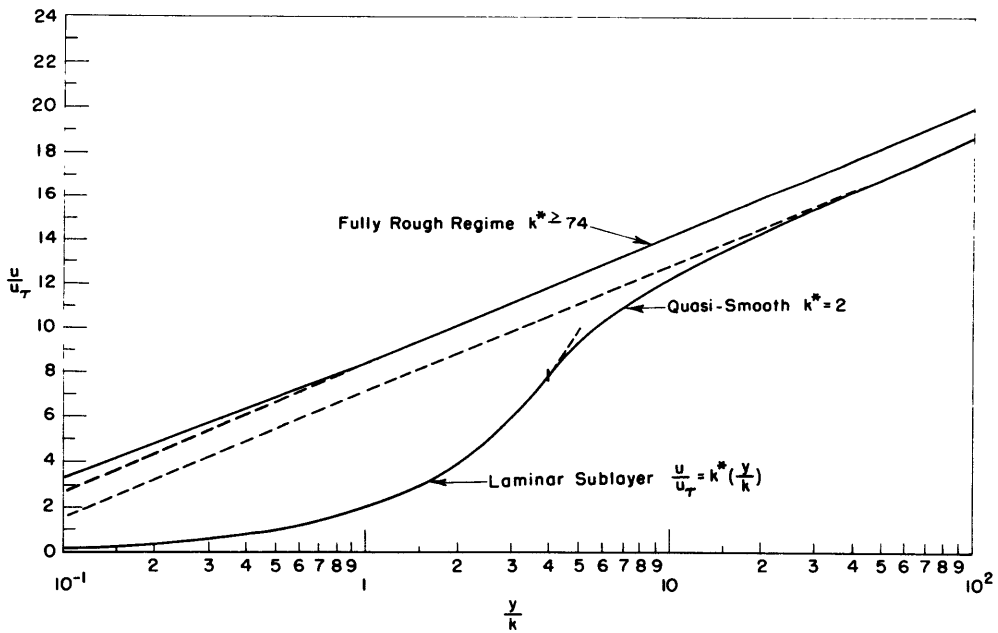


Figure 6 – Plot of Inner Law for Nikuradse's Sand Rough Pipe Data



TABLE 1

Summary of Factors for the Velocity Laws of Transitional Sublayers

Factor	Quasi-Smooth Regime $0 \leq k^* \leq k_s^*$	General Rough Regime $k_s^* < k^* < k_R^*$	Fully Rough Regime $k^* \geq k_R^*$
$B_1$	$B_{1,s}$ (const)	$f(k^*)$	$B_{2,R} - A \ln k^*$
$B_2$	$B_{1,s} + A \ln k^*$	$f(k^*)$	$B_{2,R}$ (const)
$y_L^*$	$B_{1,s} + A \ln A$	$B_1 + A \ln A =$ $B_2 + A \ln \frac{A}{k^*}$	0
$J_1$	$B_{1,s} - A \ln \frac{e}{A}$	$E_1 - A \ln \frac{e}{A} =$ $B_2 - A \ln \left( \frac{ek^*}{A} \right)$	$-k^* e^{-\frac{B_{2,R}}{A}}$
$J_2$	$\frac{1}{k^*} \left( B_{1,s} - A \ln \frac{e}{A} \right)$	$\frac{1}{k^*} \left( B_1 - A \ln \frac{e}{A} \right)$	$-e^{-\frac{B_{2,R}}{A}}$
$\frac{u}{u_\tau}$	$A \ln (y^* - J_{1,s}) + B_{1,s}$	$A \ln (y^* - J_1) + B_1 =$ $A \ln \left( \frac{y}{k} - J_2 \right) + B_2$	$A \ln \left( \frac{y}{k} - J_{2,R} \right) + B_{2,R}$

The limit of quasi-smooth flow is specified by  $k_s^*$  which is the criterion for permissible roughness. The value of  $k_s^*$  may be empirically determined at the point where  $B_1$  is substantially constant as shown in Figure 1. However, Goldstein<sup>17</sup> presents a method based on the flow separation induced by an individual roughness element.

## BOUNDARY-LAYER PARAMETERS

In order to obtain relations for the boundary-layer parameters of displacement thickness  $\delta^*$ , momentum thickness  $\theta$ , and shape parameter  $H$  from the similarity laws, integrations of the velocity  $u$  with respect to  $y$  are necessary over the boundary layer. This is accomplished piecewise for each sublayer by using the appropriate velocity law as shown in Table 2.

Since the displacement thickness  $\delta^*$  is defined as

$$\delta^* \equiv \int_0^{\delta} \left( 1 - \frac{u}{U} \right) dy \quad [54]$$

**TABLE 2**  
**Velocity Profile Integrals**

Condition	Limits	Velocity Law	$\int \frac{u}{u_T} dy^*$ or $\int \frac{u}{u_T} d\left(\frac{y}{k}\right)$	$\int \left(\frac{u}{u_T}\right)^2 dy^*$ or $\int \left(\frac{u}{u_T}\right)^2 d\left(\frac{y}{k}\right)$
Linear layer	$0 \leq y^* \leq y_L^*$	$\frac{u}{u_T} = y^*$	$\frac{1}{2} y_L^{*2}$	$\frac{1}{3} y_L^{*3}$
	$0 \leq \frac{y}{k} \leq \left(\frac{y}{k}\right)_L$	$\frac{u}{u_T} = k^* \left(\frac{y}{k}\right)$	$\frac{k^*}{2} \left(\frac{y}{k}\right)_L^2$	$\frac{k^{*2}}{3} \left(\frac{y}{k}\right)_L^3$
Logarithmic layer	$y_L^* \leq y^* \leq y_T^*$	$\frac{u}{u_T} = A \ln(y^* - J_1) + B_1$	$(y_T^* - J_1) \left(\frac{u}{u_T}\right)_T - A y_T^*$	$(y_T^* - J_1) \left[\left(\frac{u}{u_T}\right)_T - A\right]^2 - A(y_T^* - A)^2 + A^2(y_T^* - y_L^*)$
	$\left(\frac{y}{k}\right)_L \leq \frac{y}{k} \leq \left(\frac{y}{k}\right)_T$	$\frac{u}{u_T} = A \ln(y^* - J_2) + B_2$	$\left[\left(\frac{y}{k}\right)_T - J_2\right] \left(\frac{u}{u_T}\right)_T - A \left(\frac{y}{k}\right)_T$	$\left[\left(\frac{y}{k}\right)_T - J_2\right] \left[\left(\frac{u}{u_T}\right)_T - A\right]^2 - \left[\left(\frac{y}{k}\right)_L - J_2\right] \left[\left(\frac{u}{u_T}\right)_L - A\right]^2 + A^2$
Intermediate layer	$y_T^* \leq y^* \leq y_G^*$ $y_G^* = \left(\frac{y}{\delta}\right)_G \left(\frac{u_T \delta}{\nu}\right)$	$\frac{u}{u_T} = A \ln y^* + B_1$	$y_G^* \left[\left(\frac{u}{u_T}\right)_G - A\right] - y_T^* \left[\left(\frac{u}{u_T}\right)_T - A\right]$	$y_G^* \left[\left(\frac{u}{u_T}\right)_G - A\right]^2 - y_T^* \left[\left(\frac{u}{u_T}\right)_T - A\right]^2 + A^2(y_G^* - y_T^*)$
	$\left(\frac{y}{k}\right)_T \leq \frac{y}{k} \leq \left(\frac{y}{k}\right)_G$ $\left(\frac{y}{k}\right)_G = \left(\frac{y}{\delta}\right)_G \left(\frac{\delta}{k}\right)$	$\frac{u}{u_T} = A \ln \frac{y}{k} + B_2$	$\left(\frac{y}{k}\right)_G \left[\left(\frac{u}{u_T}\right)_G - A\right] - \left(\frac{y}{k}\right)_T \left[\left(\frac{u}{u_T}\right)_T - A\right]$	$\left(\frac{y}{k}\right)_G \left[\left(\frac{u}{u_T}\right)_G - A\right]^2 - \left(\frac{y}{k}\right)_T \left[\left(\frac{u}{u_T}\right)_T - A\right]^2 + A^2 \left[\left(\frac{y}{k}\right)_G - \left(\frac{y}{k}\right)_T\right]$
Intermediate layer	$\left(\frac{y}{\delta}\right)_G \leq \frac{y}{\delta} \leq 1$	$\frac{u}{u_T} = \sigma - F$	$\left(\frac{u_T \delta}{\nu}\right) \left\{ \left[1 - \left(\frac{y}{\delta}\right)_G\right] \sigma - I_1 \right\}$	$\left(\frac{u_T \delta}{\nu}\right) \left\{ \left[1 - \left(\frac{y}{\delta}\right)_G\right] \sigma^2 - 2\sigma I_1 + I_2 \right\}$
			$\frac{\delta}{k} \left\{ \left[1 - \left(\frac{y}{\delta}\right)_G\right] \sigma - I_1 \right\}$	$\frac{\delta}{k} \left\{ \left[1 - \left(\frac{y}{\delta}\right)_G\right] \sigma^2 - 2\sigma I_1 + I_2 \right\}$
Boundary layer	$0 \leq y^* \leq \frac{u_T \delta}{\nu}$		$\left(\frac{u_T \delta}{\nu}\right) (\sigma - D_1) + \alpha_1$	$\left(\frac{u_T \delta}{\nu}\right) (D_2 - 2\sigma D_1 + \sigma^2) + \alpha_1$
	$0 \leq \frac{y}{k} \leq \frac{\delta}{k}$		$\frac{\delta}{k} (\sigma - D_1) + \alpha_2$	$\frac{\delta}{k} (D_2 - 2\sigma D_1 + \sigma^2) + \beta_2$

$$I_1 = \int_{\left(\frac{y}{\delta}\right)_G}^1 F d\left(\frac{y}{\delta}\right), \quad I_2 = \int_{\left(\frac{y}{\delta}\right)_G}^1 F^2 d\left(\frac{y}{\delta}\right), \quad \alpha_1 = \frac{y_L^{*2}}{2} - J_1 \left(\frac{u}{u_T}\right), \quad \alpha_2 = \frac{\alpha_1}{k^*}, \quad D_1 = \left(\frac{y}{\delta}\right)_G (F_G + A) + I_1$$

$$\beta_1 = \frac{y_L^{*3}}{3} - J_1 \left[\left(\frac{u}{u_T}\right) - A\right]^2 - A(y_L^{*2} - A y_L^* + A^2), \quad \beta_2 = \frac{\beta_1}{k^*}, \quad D_2 = \left(\frac{y}{\delta}\right)_G \left[(F_G + A)^2 + A^2\right] + I_2$$

then from the integrated quantities from the similarity laws in Table 2

$$\frac{\delta^*}{\delta} = \frac{1}{\sigma} \left( D_1 - \frac{\alpha_1}{\frac{u_\tau \delta}{\nu}} \right) = \frac{1}{\sigma} \left( D_1 - \frac{\alpha_2}{\frac{\delta}{k}} \right) \quad [55]$$

$$\frac{U\delta^*}{\nu} = D_1 \left( \frac{u_\tau \delta}{\nu} \right) - \alpha_1 \quad [56]$$

and

$$\frac{\delta^*}{k} = \frac{1}{\sigma} \left( D_1 \frac{\delta}{k} - \alpha_2 \right) \quad [57]$$

In a like manner for momentum thickness  $\theta$  defined as

$$\theta \equiv \int_0^\delta \frac{u}{U} \left( 1 - \frac{u}{U} \right) dy \quad [58]$$

$$\frac{\theta}{\delta} = \frac{1}{\sigma} \left( D_1 + \frac{\alpha_1}{\frac{u_\tau \delta}{\nu}} \right) - \frac{1}{\sigma^2} \left( D_2 + \frac{\beta_1}{\frac{u_\tau \delta}{\nu}} \right) \quad [59]$$

$$\frac{\theta}{\delta} = \frac{1}{\sigma} \left( D_1 + \frac{\alpha_2}{\frac{\delta}{k}} \right) - \frac{1}{\sigma^2} \left( D_2 + \frac{\beta_2}{\frac{\delta}{k}} \right) \quad [60]$$

$$R_\theta \equiv \frac{U\theta}{\nu} = \frac{u_\tau \delta}{\nu} \left( D_1 - \frac{D_2}{\sigma} \right) + \alpha_1 - \frac{\beta_1}{\sigma} \quad [61]$$

and

$$\frac{\theta}{k} = \frac{\delta}{k} \left( \frac{D_1}{\sigma} - \frac{D_2}{\sigma^2} \right) + \frac{\alpha_2}{\sigma} - \frac{\beta_2}{\sigma^2} \quad [62]$$

Also for shape parameter  $H$  defined as

$$H \equiv \frac{\delta^*}{\theta} \quad [63]$$

$$\frac{1}{H} = 1 - \frac{1}{\sigma} \left[ \frac{D_2 + \frac{\beta_1 - 2\sigma\alpha_1}{\frac{u_T \delta}{\nu}}}{D_1 - \frac{\alpha_1}{\frac{u_T \delta}{\nu}}} \right] \quad [64]$$

or

$$\frac{1}{H} = 1 - \frac{1}{\sigma} \left[ \frac{D_2 + \frac{\beta_2 - 2\sigma\alpha_2}{\delta/k}}{D_1 - \frac{\alpha_2}{\delta/k}} \right] \quad [65]$$

Since  $\frac{u_T \delta}{\nu}$  and  $\frac{\delta}{k}$  are given in terms of  $\sigma$  in Equations [11] and [12],  $\delta^*$ ,  $\theta$ , and  $H$  are functions of  $\sigma$  according to the preceding relationships.

For zero pressure gradient the factors  $D_1$  and  $D_2$  are constant for the three types of roughness flow. However,  $B_1$ ,  $\alpha_1$ , and  $\beta_1$  are constant only for the quasi-smooth regime while  $B_2$ ,  $\alpha_2$ , and  $\beta_2$  are constant only for the fully rough regime. In the case of the general rough regime  $B_1$ ,  $B_2$ ,  $\alpha_1$ ,  $\alpha_2$ ,  $\beta_1$ , and  $\beta_2$  are all functions of  $k^*$ .

## FRICTIONAL RESISTANCE OF FLAT PLATES

### GENERAL

The frictional resistance or drag of a flat plate in two-dimensional flow without pressure gradients which corresponds to a flat plate moving lengthwise in an infinite fluid is determined by the momentum thickness of the boundary-layer flow leaving the trailing edge as a wake. The Von Kármán momentum equation neglecting the small effect of the normal Reynolds stress term gives<sup>1</sup>

$$\frac{d\theta}{dx} = \frac{\tau_w}{\rho U^2} \quad [66]$$

and since the resistance coefficient  $C_f \equiv \frac{R_f}{\frac{1}{2} \rho U^2 x b}$ , where  $R_f$  is the total frictional resistance

on one side and  $b$  the width of the plate, is obtained from the summation of the local resistance

or

$$\frac{C_f}{2} = \frac{1}{x} \int_0^x \frac{\tau_w}{\rho U^2} dx \quad [67]$$

then

$$\frac{C_f}{2} = \frac{\theta}{x} = \frac{R_\theta}{R_x} = \frac{\frac{\theta}{k}}{\frac{x}{k}} \quad [68]$$

where  $R_x \equiv \frac{Ux}{\nu}$ .

Since by definition

$$\sigma^2 \equiv \frac{1}{\frac{\tau_w}{\rho U^2}} \quad [69]$$

then Equation [66] becomes

$$dx = \sigma^2 d\theta \quad [70]$$

or

$$dR_x = \sigma^2 dR_\theta \quad [71]$$

or

$$d\left(\frac{x}{k}\right) = \sigma^2 d\left(\frac{\theta}{k}\right) \quad [72]$$

For a uniform roughness where  $k$  is constant with respect to  $x$

$$R_x = \int \sigma^2 dR_\theta = \sigma^2 R_\theta - 2 \int R_\theta \sigma d\sigma + \text{const} \quad [73]$$

or

$$\frac{x}{k} = \int \sigma^2 d\left(\frac{\theta}{k}\right) = \sigma^2 \frac{\theta}{k} - 2 \int \frac{\theta}{k} \sigma d\sigma + \text{const} \quad [74]$$

The general case of the frictional resistance of a rough plate is to be now considered wherein  $B_1$  or  $B_2$  is an unspecified function of  $k^*$ . All other cases like that of the fully rough regime or the quasi-smooth regime are then special cases.

Inserting the relation  $\frac{\delta}{k}$  from Equation [12] into the relation for  $\frac{\theta}{k}$  from Equation [62] and integrating by parts repeatedly results in

$$\int \frac{\theta}{k} \sigma d\sigma = \frac{\delta}{k} \left\{ AD_1 \left[ 1 - \frac{B_2'}{\sigma} - \frac{A}{\sigma^2} \left( B_2' + B_2'' - \frac{B_2'^2}{A} \right) + \dots \right] - \frac{AD_2}{\sigma} \left[ 1 + \frac{(A - B_2')}{\sigma} + \dots \right] \right\} ,$$

$$+ \int \alpha_2 d\sigma - \int \frac{\beta_2}{\sigma} d\sigma + \text{const} \quad [75]$$

where

$$B_2' \equiv \frac{dB_2}{d(\ln k^*)} \quad [76]$$

and

$$B_2'' \equiv \frac{d^2 B_2}{d(\ln k^*)^2} \quad [77]$$

Then from Equation [74]

$$\frac{x}{k} = \frac{\delta}{k} \left\{ D_1 \sigma - D_2 - 2AD_1 \left[ 1 - \frac{B_2'}{\sigma} - \frac{A}{\sigma^2} \left( B_2' + B_2'' - \frac{B_2'^2}{A} \right) + \dots \right] + \frac{2AD_2}{\sigma} \left[ 1 + \frac{(A - B_2')}{\sigma} + \dots \right] \right\}$$

$$+ \alpha_2 \sigma - \beta_2 - 2 \int \alpha_2 d\sigma + 2 \int \frac{\beta_2}{\sigma} d\sigma + \text{const} \quad [78]$$

Also since by definition

$$\frac{x}{k} \equiv \frac{R_x}{\sigma k^*} = \frac{R_x}{\sigma} \frac{\delta}{k} \quad [79]$$

Equation [78] becomes then

$$R_x = \frac{u_r \delta}{\nu} \left\{ D_1 \sigma^2 - D_2 \sigma - 2AD_1 \sigma \left[ 1 - \frac{B_2'}{\sigma} - \frac{A}{\sigma^2} \left( B_2' + B_2'' - \frac{B_2'^2}{A} \right) + \dots \right] + 2AD_2 \left[ 1 + \frac{(A - B_2')}{\sigma} + \dots \right] \right\} \quad [80]$$

$$+ \alpha_1 \sigma^2 - \beta_1 \sigma - 2 \int \alpha_1 \sigma d\sigma + 2 \int \beta_1 d\sigma + \text{const}$$

Hence from Equation [68] it is seen that  $C_f$  is a function of  $R_x$  and/or  $\frac{x}{k}$  in terms of parameter  $\sigma$ . When  $\sigma$  is eliminated, logarithmic resistance formulas result. To arrive at a relation between  $C_f$  and  $\sigma$ , Equations [68] and [73] or [74] are combined to give after neglecting the constant of integration

$$\frac{1}{\sigma^2} = \frac{C_f}{2} \left( 1 - \frac{2 \int R \theta \sigma d\sigma}{\sigma^2 R \theta} \right) \quad [81]$$

or

$$\frac{1}{\sigma^2} = \frac{C_f}{2} \left( 1 - \frac{2 \int \frac{\theta}{k} \sigma d\sigma}{\sigma^2 \frac{\theta}{k}} \right) \quad [82]$$

The expressions for  $\int \frac{\theta}{k} \sigma d\sigma$  and  $\frac{\theta}{k}$  from Equations [75] and [62] are inserted into Equation [82] to give with  $\alpha_2$  and  $\beta_2$  neglected:

$$\frac{1}{\sigma^2} = \frac{C_f}{2} \left[ 1 - \frac{2A}{\sigma} + \frac{2AB_2'}{\sigma^2} + \frac{2A^2}{\sigma^3} \left( B_2' + B_2'' - \frac{B_2'^2}{A} + \frac{D_2}{D_1} \right) + \dots \right] \quad [83]$$

Through reiteration  $\sigma$  is replaced by  $C_f$  within the brackets so that

$$\frac{1}{\sigma^2} = \frac{C_f}{2} \left[ 1 - 2A \left( \frac{C_f}{2} \right)^{\frac{1}{2}} + 2A \left( A + B_2' \right) \left( \frac{C_f}{2} \right) + \dots \right] \quad [84]$$

and by the binomial expansion

$$\frac{1}{\sigma} = \sqrt{\frac{C_f}{2}} \left[ 1 - A \left( \frac{C_f}{2} \right)^{\frac{1}{2}} + A \left( \frac{A}{2} + B_2' \right) \left( \frac{C_f}{2} \right) + \dots \right] \quad [85]$$

and by inversion

$$\sigma = \sqrt{\frac{2}{C_f}} \left[ 1 + A \left( \frac{C_f}{2} \right)^{\frac{1}{2}} + A \left( \frac{A}{2} - B'_2 \right) \left( \frac{C_f}{2} \right) + \dots \right] \quad [86]$$

Now, after substituting for  $\frac{\delta}{k}$  from Equation [12] and eliminating  $\alpha_2$ ,  $\beta_2$ , and the constant of integration,  $\frac{x}{k}$  in Equation [78] is written in logarithmic form as

$$\ln \frac{x}{k} = \frac{\sigma}{A} - \frac{B_3}{A} - \frac{B_2}{A} + \ln D_1 - \ln \frac{1}{\sigma} + \ln \left[ 1 - \left( 2A + \frac{D_2}{D_1} \right) \frac{1}{\sigma} + \dots \right] \quad [87]$$

Substituting the appropriate expressions for  $\sigma$  from Equations [85] and [86] and expanding the logarithm of terms close to unity into a series results in

$$\ln \frac{x}{k} \sqrt{C_f} = \frac{\sqrt{2}}{A} \frac{1}{\sqrt{C_f}} - \frac{1}{\sqrt{2}} \left( \frac{A}{2} + \frac{D_2}{D_1} + B'_2 \right) \sqrt{C_f} + 1 - \frac{B_3}{A} - \frac{B_2}{A} + \ln \sqrt{2} D_1 \quad [88]$$

wherein terms of higher order than  $\sqrt{C_f}$  have been neglected. Inserting the expression for  $\frac{x}{k}$  from Equation [79] and  $\frac{1}{\sigma}$  from Equation [85] into [88] produces

$$\ln R_x C_f = \frac{\sqrt{2}}{A} \frac{1}{\sqrt{C_f}} - \frac{1}{\sqrt{2}} \left( \frac{D_2}{D_1} - \frac{A}{2} + B'_2 \right) \sqrt{C_f} + 1 - \frac{B_3}{A} - \frac{B_1}{A} + \ln 2 D_1 \quad [89]$$

Equations [88] and [89] represent logarithmic resistance formulas for the general case of constant  $k^*$  since  $B_1$  and  $B_2$  are functions of  $k^*$ . Separate logarithmic formulas are obtained from Equations [88] or [89] in the cases where  $B_1$  or  $B_2$  is analytically defined in terms of  $\ln k^*$ .

## FULLY ROUGH REGIME

In this case the roughness effects have become strong enough to eliminate the laminar sublayer and make  $B_2$  constant. With  $B_2 = B_{2,R}$  and  $B'_2 = 0$ , Equation [88] reduces to

$$\ln \frac{x}{k} \sqrt{C_f} = \frac{\sqrt{2}}{A} \frac{1}{\sqrt{C_f}} - \frac{1}{\sqrt{2}} \left( \frac{A}{2} + \frac{D_2}{D_1} \right) \sqrt{C_f} + 1 - \frac{B_3}{A} - \frac{B_{2,R}}{A} + \ln \sqrt{2} D_1 \quad [90]$$

If the term involving  $\sqrt{C_f}$  is linearized with respect to  $\frac{1}{\sqrt{C_f}}$

or

$$\sqrt{C_f} = C_1 + \frac{C_2}{\sqrt{C_f}} \quad [91]$$



then Equation [90] becomes in common logarithms

$$\log_{10} \frac{x}{k} \sqrt{C_f} = \frac{M_1}{\sqrt{C_f}} + N_1 \quad [92]$$

where

$$M_1 = \frac{1}{2.3026} \left[ \frac{\sqrt{2}}{A} - \left( \frac{A}{2} + \frac{D_2}{D_1} \right) \frac{C_2}{\sqrt{2}} \right] \quad [93]$$

and

$$N_1 = \frac{1}{2.3026} \left[ 1 - \left( \frac{A}{2} + \frac{D_2}{D_1} \right) \frac{C_1}{\sqrt{2}} - \frac{(B_3 + B_{2,R})}{A} \right] + \log_{10} \sqrt{2} D_1 \quad [94]$$

Furthermore, if  $\log_{10} C_f$  is linearized with respect to  $\frac{1}{\sqrt{C_f}}$

or

$$\log_{10} C_f = C_3 + \frac{C_4}{\sqrt{C_f}} \quad [95]$$

then Equation [92] becomes

$$\log_{10} \frac{x}{k} = \frac{M_2}{\sqrt{C_f}} + N_2 \quad [96]$$

or

$$C_f = \frac{M_2^2}{\left( \log_{10} \frac{x}{k} - N_2 \right)^2} \quad [97]$$

where

$$M_2 = M_1 - \frac{C_4}{2} \quad [98]$$

and

$$N_2 = N_1 - \frac{C_3}{2} \quad [99]$$

## QUASI-SMOOTH REGIME

Quasi-smooth flow is effectively that of a smooth surface;  $B_1$  being constant and equal to  $B_{1,s}$  and  $\frac{dB_1}{d \ln k^*} = 0$ .

Since, from Equation [9]

$$B_2' = \frac{dB_2}{d \ln k^*} = \frac{dB_1}{d \ln k^*} + A \quad [100]$$

Equation [89] reduces to

$$\ln R_x C_f = \frac{\sqrt{2}}{A} \frac{1}{\sqrt{C_f}} - \frac{1}{\sqrt{2}} \left( \frac{A}{2} + \frac{D_2}{D_1} \right) \sqrt{C_f} + 1 - \frac{B_3}{A} - \frac{B_{1,s}}{A} + \ln 2 D_1 \quad [101]$$

If the term involving  $\sqrt{C_f}$  is linearized with respect to  $\frac{1}{\sqrt{C_f}}$  as in Equation [91], Equation [101] becomes in common logarithms

$$\log_{10} R_x C_f = \frac{M_1}{\sqrt{C_f}} + N_1' \quad [102]$$

where  $M_1$  is given by Equation [93] and

$$N_1' = N_1 + \frac{B_{2,R} - B_{1,s}}{2.3026A} + \log_{10} \sqrt{2} \quad [103]$$

Equation [102] is the well-known Kármán-Schoenherr formula which is derived in Reference 20 by a somewhat different procedure.

If  $\log_{10} C_f$  is linearized with respect to  $\frac{1}{\sqrt{C_f}}$  as indicated in Equation [95], Equation [102] becomes

$$\log_{10} R_x = \frac{M_2'}{\sqrt{C_f}} + N_2' \quad [104]$$

or

$$C_f = \frac{(M_2')^2}{(\log_{10} R_x - N_2')^2} \quad [105]$$

where

$$M_2' = M_1 - C_4 \quad [106]$$

and

$$N_2' = N_1' - C_3 \quad [107]$$

## ENGINEERING ROUGHNESS

From extensive tests on commercial pipes the behavior of the irregular roughness of the surfaces resulting from manufacturing processes, termed here engineering roughness, has been found to be quite different from that of the artificial sand roughness of Nikuradse.

Whereas  $B_2$  has a maximum value for the Nikuradse roughness,  $B_2$  has a gradual monotonic variation for engineering roughness as shown in Figure 1. Colebrook<sup>19</sup> with the aid of White fitted this variation of  $B_2$  with the following formula which in the notation of this paper can be expressed as

$$B_2 = B_{2,R} - A \ln \left( 1 + \frac{\lambda}{k^*} \right) \quad [108]$$

where

$$\lambda = \exp \left[ \frac{1}{A} (B_{2,R} - B_{1,s}) \right] \quad [109]$$

It is seen that for  $k^* \rightarrow \infty$ ,  $B_2 \rightarrow B_{2,R}$ .

Furthermore, with Equation [9], [108] becomes

$$B_1 = B_{1,s} - A \ln \left( 1 + \frac{k^*}{\lambda} \right) \quad [110]$$

Then for  $k^* \rightarrow 0$ ,  $B_1 \rightarrow B_{1,s}$ . Consequently the relation for engineering roughness is asymptotic to both the quasi-smooth regime and the fully rough regime.

To obtain a logarithmic resistance formula for engineering roughness from Equation [89], the procedure is as follows:

From Equation [108]

$$B_2' = \frac{A}{1 + \frac{\lambda}{k^*}} \quad [111]$$

Now from Equations [79] and [85]

$$1 + \frac{k^*}{\lambda} = 1 + \frac{R_x}{\lambda \frac{x}{k}} \sqrt{\frac{C_f}{2}} \left( 1 - A \sqrt{\frac{C_f}{2}} + \dots \right) = \left( 1 + \frac{R_x}{\lambda \frac{x}{k}} \right) \sqrt{\frac{C_f}{2}} \left[ 1 - \frac{\left( \frac{A R_x}{\lambda \frac{x}{k}} \right) \left( \frac{C_f}{2} \right)}{1 + \left( \frac{R_x}{\lambda \frac{x}{k}} \right) \left( \frac{C_f}{2} \right)^{1/2}} + \dots \right] \quad [112]$$

Using Equations [110], [111], and [112] in [89] results in

$$-\ln \left( \frac{1}{R_x C_f} + \frac{1}{\sqrt{2} \lambda \frac{x}{k} \sqrt{C_f}} \right) = \frac{\sqrt{2}}{A} \frac{1}{\sqrt{C_f}} - \frac{1}{\sqrt{2}} \left( \frac{A}{2} + \frac{D_2}{D_1} \right) \sqrt{C_f} + 1 - \frac{B_3}{A} - \frac{B_{1,s}}{A} + \ln 2 D_1 \quad [113]$$

If the term containing  $\sqrt{C_f}$  is linearized with respect to  $\frac{1}{\sqrt{C_f}}$  as in Equation [91], Equation [113] becomes in common logarithms

$$-\log_{10} \left( \frac{1}{R_x C_f} + \frac{1}{\sqrt{2} \lambda \frac{x}{k} \sqrt{C_f}} \right) = \frac{M_1}{\sqrt{C_f}} + N_1' \quad [114]$$

where  $M_1$  is given by Equation [93] and  $N_1'$  by Equation [103].

Equation [114] reduces to the case for smooth flow, Equation [102], when

$$\frac{1}{\sqrt{2} \lambda \frac{x}{k} \sqrt{C_f}} \rightarrow 0 \text{ and to the case for the fully rough regime, Equation [92], when } \frac{1}{R_x C_f} \rightarrow 0.$$

In a less rigorous fashion an explicit expression between  $C_f$  and  $R_x$  and  $\frac{x}{k}$  may be written which agrees in the limits with Equation [104] for the quasi-smooth regime and with Equation [96] for the fully rough regime or

$$-\log_{10} \left[ \frac{1}{R_x} + \frac{1}{\left( \frac{x}{k} \right)^m} \right] = \frac{M_2'}{\sqrt{C_f}} + N_2' \quad [115]$$

where  $M_2'$  and  $N_2'$  are given in Equations [106] and [107],

$$\log_{10} \gamma = \frac{N_2' M_2'}{M_2'} - N_2' \quad [116]$$

and

$$m = \frac{M_2'}{M_2} \quad [117]$$

## APPLICATION OF THE GENERAL LOGARITHMIC RESISTANCE FORMULA TO ARBITRARY ROUGHNESS

### PREPARATION OF RESISTANCE DIAGRAMS FROM RESISTANCE CHARACTERIZATIONS

If the resistance characterization is known for an arbitrary roughness, e.g.,  $B_1$  or  $B_2$  has been found empirically as a function of  $k^*$ , the procedure for preparing a resistance diagram for flat plates,  $C_f$  as a function of  $R_x$  and  $x/k$ , is as follows:

The general logarithmic resistance formula, Equation [89], is restated in common logarithms and Equation [100] substituted for  $B_2'$

$$\log_{10} R_x C_f = \frac{\sqrt{2}}{2.3026A} \frac{1}{\sqrt{C_f}} - \frac{\sqrt{C_f}}{2.3026\sqrt{2}} \left( \frac{A}{2} + \frac{D_2}{D_1} + \frac{1}{2.3026} \frac{dB_1}{d\log_{10} k^*} \right) + \frac{1}{2.3026} \left( 1 - \frac{B_3}{A} - \frac{B_1}{A} \right) \quad [118]$$

$$+ \log_{10} 2 D_1$$

Since  $B_1$  and  $\frac{dB_1}{d\log_{10} k^*}$  are functions of  $k^*$  and  $A$ ,  $B_3$ ,  $D_1$ , and  $D_2$  are constants, Equation [118] represents the variation of  $C_f$  with  $R_x$  for constant  $k^*$ . A rapid method of plotting Equation [118] is to relate it to smooth resistance so that for the same value of  $C_f$  the difference in  $R_x$  is

$$\log_{10} R_x - \log_{10} R_{x,s} = \frac{B_{1,s} - B_1}{2.3026A} \quad [119]$$

where the effect due to  $\frac{dB_1}{d\log_{10} k^*}$  is neglected and the subscript  $s$  refers to the smooth line.

Consequently the resistance line of constant  $k^*$  for the rough case is offset from the smooth line by a constant amount in the direction of  $\log_{10} R_x$ .

To determine the resistance lines of constant  $x/k$  from the lines of constant  $k^*$  the following procedure is used:

Since by definition

$$R_x \equiv k^* \sigma \frac{x}{k} \quad [120]$$

the insertion of the relation for  $\sigma$  from Equation [86] produces

$$R_x = k^* \frac{x}{k} \sqrt{\frac{2}{C_f}} \left( 1 + A \sqrt{\frac{C_f}{2}} + \dots \right) \quad [121]$$

Taking the common logarithm of Equation [121] and expanding the logarithm of the series in parentheses results in

$$\log_{10} R_x = \log_{10} k^* + \log_{10} \sqrt{\frac{2}{C_f}} + \frac{A}{2.3026} \sqrt{\frac{C_f}{2}} + \log_{10} \frac{x}{k} \quad [122]$$

wherein terms of higher order than  $\sqrt{C_f}$  have been neglected. Hence for a given  $k^*$  and  $x/k$  the intersection of Equation [122] and [119] at a specified  $k^*$  gives a point on the line of constant  $x/k$ . A rapid way of plotting other lines of Equation [122] is to relate them to any plotted line of Equation [122] at constant  $C_f$  or

$$\log_{10} R_{x,2} - \log_{10} R_{x,1} = \log_{10} k_2^* - \log_{10} k_1^* + \log_{10} \left( \frac{x}{k} \right)_2 - \log_{10} \left( \frac{x}{k} \right)_1 \quad [123]$$

where subscript 2 refers to the new line and subscript 1 to the line already plotted. Hence the various plots of Equation [122] are offset by constant amounts in the direction of  $\log_{10} R_x$ .

This procedure was utilized in preparing the resistance diagram for sand roughness in Figure 7 from a graphical representation of  $B_1$  and  $k^*$ .

## RESISTANCE CHARACTERIZATIONS FROM PLATE TESTS

To characterize the resistance qualities of an arbitrary roughness requires the determination of  $B_1$  or  $B_2$  as a function of  $k^*$ . Measurements of total resistance of flat plates with an arbitrarily rough surface can only give values of  $C_f$  against  $R_x$  for different lengths  $x$ , the roughness parameter  $k$  having only meaning for a particular roughness configuration. Hence to compare the resistance characterizations of different roughnesses from measurements of total resistance of flat plates, it is necessary to use the following procedure:

A new parameter  $x^*$  is introduced where

$$x^* \equiv \frac{u_\tau x}{\nu} \quad [124]$$

so that by definition

$$k^* \equiv \frac{x^*}{x/k} \quad [125]$$

or

$$\log_{10} k^* = \log_{10} x^* - \log_{10} \frac{x}{k} \quad [126]$$

Then the single parameter variation of  $B_1$  with  $k^*$  is replaced by a two-parameter variation of  $B_1$  with  $x^*$  and  $x/k$ . Consequently when  $B_1$  is plotted against  $\log_{10} x^*$ , a family of curves result for different values of  $x/k$  which are offset by constant amounts of the differences in  $\log_{10} x/k$ .

$B_1$  is determined from the general logarithmic resistance formula [118] and from the fact that for constant  $x/k$

$$\frac{dB_1}{d \log_{10} k^*} = \frac{dB_1}{d \log_{10} x^*} \quad [127]$$

or

$$B_1 = \sqrt{\frac{2}{C_f}} - \frac{A}{\sqrt{2}} \left( \frac{A}{2} + \frac{D_2}{D_1} + \frac{1}{2.3026} \frac{dB_1}{d \log_{10} x^*} \right) \sqrt{C_f} + A - B_3 + 2.3026A \log_{10} \left( \frac{2D_1}{R_x C_f} \right) [128]$$

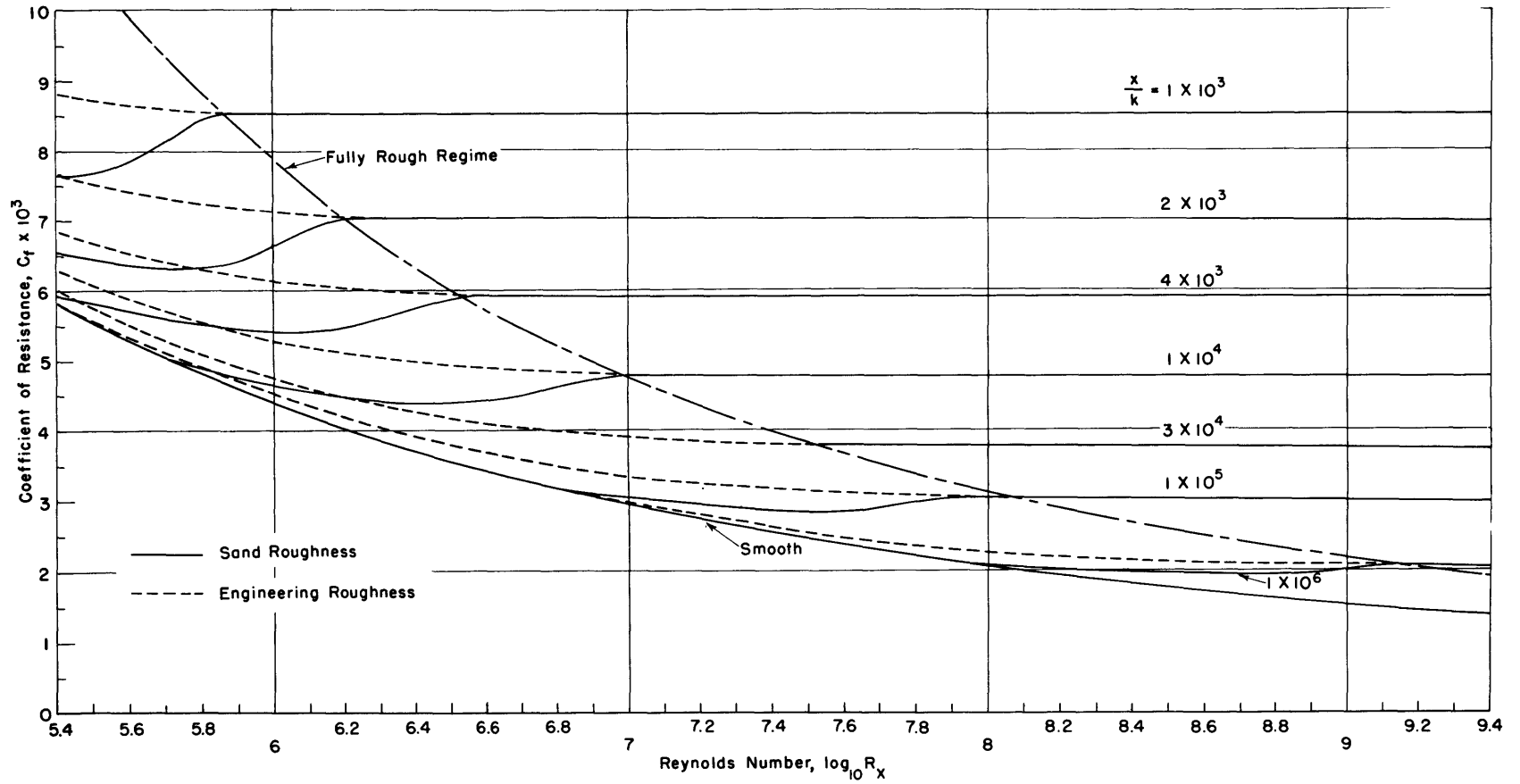


Figure 7 – Resistance Diagram for Rough Plates with Sand Roughness and Engineering Roughness

or relative to the smooth line for the same  $C_f$

$$B_1 = B_{1,s} - \frac{A}{2.3026} \frac{dB_1}{d \log_{10} x^*} \sqrt{\frac{C_f}{2}} - 2.3026A (\log_{10} R_x - R_{x,s}) \quad [129]$$

The small effect due to  $\frac{dB_1}{d \log_{10} x^*}$  can be evaluated by iteration.

Since by definition

$$x^* = \frac{R_x}{\sigma} \quad [130]$$

then substituting for  $1/\sigma$  from Equation [85] and manipulating the logarithm of the series gives

$$\log_{10} x^* = \log_{10} R_x + \log_{10} \sqrt{\frac{C_f}{2}} - \frac{A}{2.3026} \sqrt{\frac{C_f}{2}} \quad [131]$$

Hence  $B_1$  and  $x^*$  can be obtained from test data of  $C_f$  against  $R_x$ .

For the same roughness  $k$  and different lengths of plate  $x$ , plots of  $B_1$  against  $\log_{10} x^*$  will be represented by curves offset by a constant amount given by the logarithm of the ratio of the lengths of the plates. Hence, if the similarity laws hold, the curves can be collapsed to a single line by parallel shifts of the curves in the  $x^*$  direction.

A resistance characterization was obtained from the data of 21-foot friction planes coated with Mare Island hot plastic paint as shown in Figure 8. For comparison the curve of engineering roughness, Equation [110], is plotted for  $x/k = 1 \times 10^5$ . The difference in curvature between the two graphs is evident.

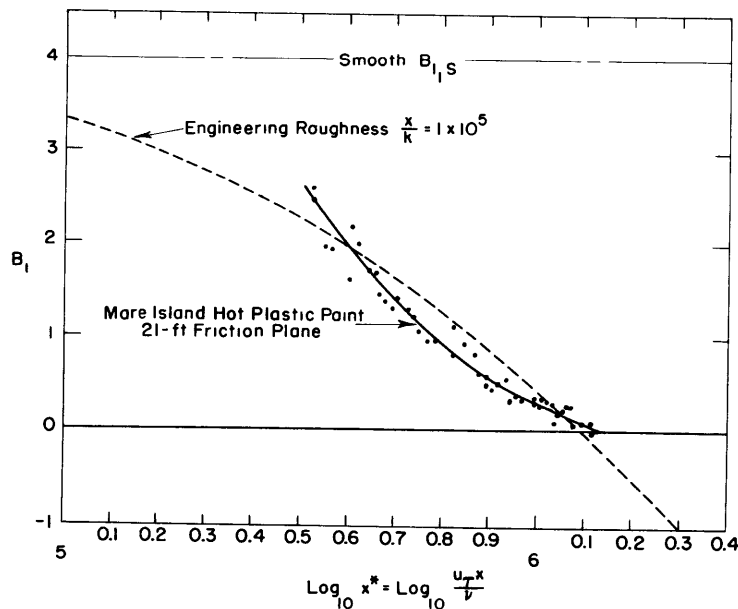


Figure 8 – Resistance Characterization of Roughness from Flat Plate Resistance Data



## PREDICTION OF FULL-SCALE RESISTANCE FROM PLATE TESTS

The general logarithmic resistance law provides a means of extrapolating data from test planks with arbitrary rough surfaces to full-scale lengths. The test data are in the form of  $C_f$  against  $\log R_x$  at constant  $x/k$ ,  $k$  being unknown. A representative plot for Mare Island hot plastic paint<sup>21</sup> is shown in Figure 9. The problem is to obtain a plot of  $C_f$  against  $\log R_x$  for different lengths of flat plates with the same roughness in order to predict the full-scale resistance of ships having that roughness.

According to the similarity laws there is a unique relationship between  $B_1$  and  $k^*$  characteristic of the roughness configuration. Hence each point of the test data or faired test curve represents a value of  $B_1$  or  $k^*$ . This is illustrated by point  $P_1$  in Figure 9 where a line of constant  $B_1$  or  $k^*$  is drawn through it by means of Equation [119] which simply requires that a constant distance from the smooth curve be maintained in the  $\log_{10} R_x$  direction. The next step is to locate a point on this line which corresponds to the desired length of plate.

First from Equation [131] a line of  $C_f$  against  $R_x$  at constant  $x^*$  is drawn using any convenient value of  $x^*$ . From Equation [131] again it is seen that at constant  $C_f$  the difference in lines at different  $x^*$  is given by

$$\log_{10} R_{x,2} - \log_{10} R_{x,1} = \log_{10} x_2^* - \log_{10} x_1^* \quad [132]$$

Since by definition

$$x^* \equiv k^* \frac{x}{k} \quad [133]$$

Equation [132] becomes for constant  $k^*$  and  $k$

$$\log_{10} R_{x,2} - \log_{10} R_{x,1} = \log_{10} \frac{x_2}{x_1} \quad [134]$$

Consequently point  $P_2$  for the new length  $x_2$  is located by a line which is at a distance of  $\log_{10} \frac{x_2}{x_1}$  from  $P_1$  and drawn a constant distance from the reference line for constant  $x^*$ . This process is repeated for enough points from the test data to draw the predicted line for the desired length as illustrated in Figure 9.

If a representative sample of the rough surface can be obtained on a test plate, it is then possible to make full-scale predictions for any arbitrary roughness configuration without regard to geometrical characterization.

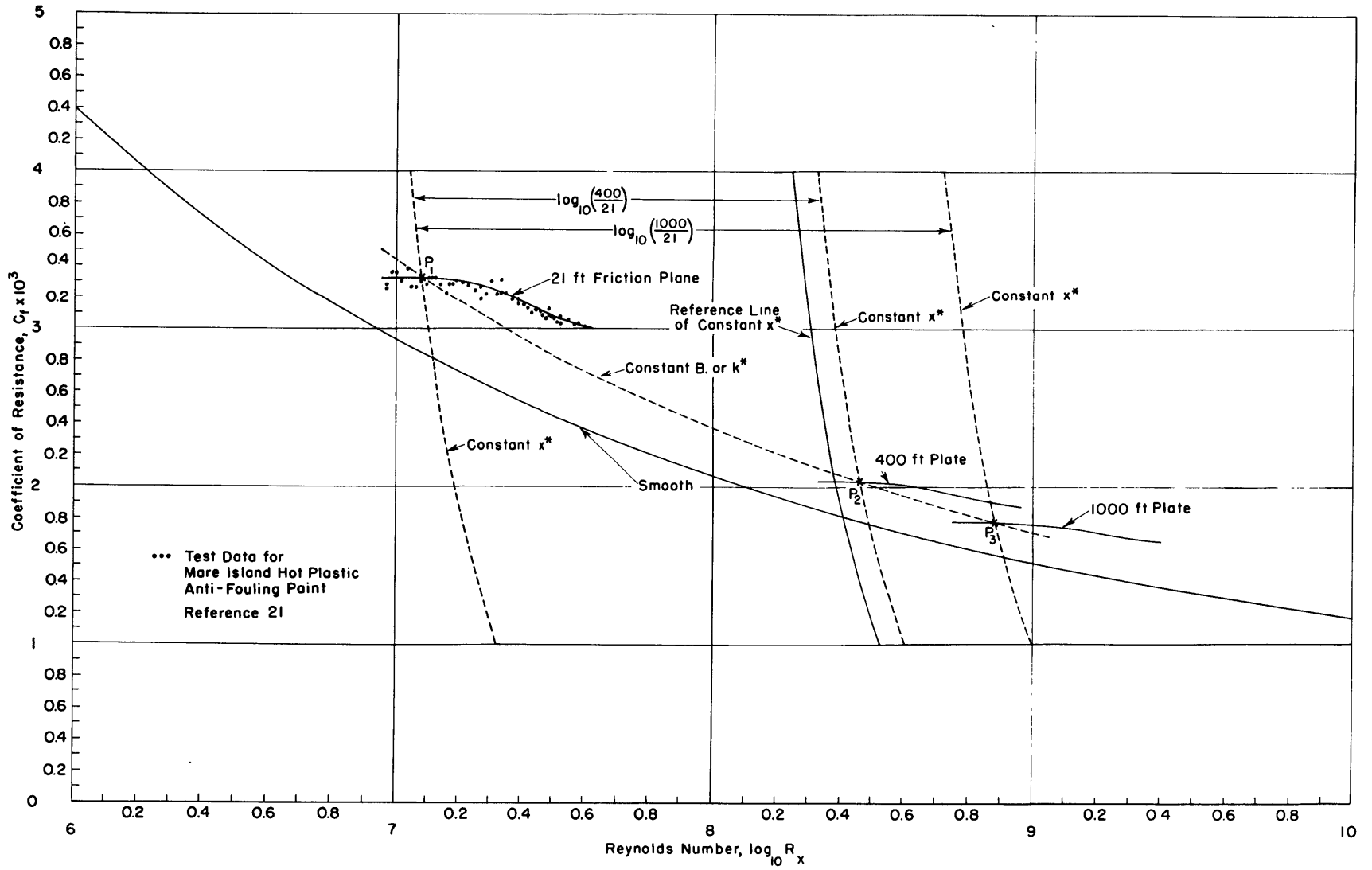


Figure 9 – Resistance Prediction Diagram for Rough Plates

## LOCAL SKIN FRICTION COEFFICIENTS AND SHAPE PARAMETERS

### GENERAL

In the calculation of turbulent boundary layers in pressure gradients to obtain the viscous resistance or separation point of foils and bodies of revolution,<sup>22, 23</sup> relations are required for the local skin friction and shape parameter as functions of momentum thickness. For rough surfaces in general the local skin friction is expressed as

$$\frac{1}{\sigma^2} \equiv \frac{C_f}{2} \equiv \frac{\tau_w}{\rho U^2} = f(R_\theta, \theta/k) \quad [135]$$

and the shape parameter  $H$  as

$$H = f(R_\theta, \theta/k) \quad [136]$$

From Equations [11] and [61] the local skin friction is expressed implicitly as

$$R_\theta = D_1 \left( 1 - \frac{D_2}{D_1 \sigma} \right) \exp \left[ \frac{1}{A} (\sigma - B_3 - B_1) \right] \quad [137]$$

or from Equation [12] and [62]

$$\frac{\theta}{k} = \frac{D_1}{\sigma} \left( 1 - \frac{D_2}{D_1 \sigma} \right) \exp \left[ \frac{1}{A} (\sigma - B_3 - B_2) \right] \quad [138]$$

where  $\alpha_1$ ,  $\beta_1$ ,  $\alpha_2$ , and  $\beta_2$  have been neglected. Logarithmically Equation [137] becomes

$$\ln R_\theta = \frac{1}{A} \sqrt{\frac{\rho U^2}{\tau_w}} - \frac{B_3}{A} - \frac{B_1}{A} + \ln D_1 - \frac{D_2}{D_1} \sqrt{\frac{\tau_w}{\rho U^2}} \quad [139]$$

and Equation [138] becomes

$$\ln \frac{\theta}{k} = \frac{1}{A} \sqrt{\frac{\rho U^2}{\tau_w}} - \frac{B_3}{A} - \frac{B_2}{A} + \ln D_1 + \ln \sqrt{\frac{\tau_w}{\rho U^2}} - \frac{D_2}{D_1} \sqrt{\frac{\tau_w}{\rho U^2}} \quad [140]$$

wherein one term has been retained in the series expansion of  $\ln \left( 1 - \frac{D_2}{D_1 \sigma} \right)$ . Equations

[139] and [140] represent the general case with  $B_1$  and  $B_2$  as functions of  $k^*$ .

In the case of shape parameter  $H$ , Equation [64] is simplified to

$$\frac{H}{H-1} = \frac{D_1}{D_2} \sigma = \frac{D_1}{D_2} \sqrt{\frac{\rho U^2}{\tau_w}} \quad [141]$$

by dropping  $\alpha_1$  and  $\beta_1$ .

## FULLY ROUGH REGIME

Since in the case of the fully rough regime  $B_2$  is constant,  $B_2 = B_{2,R}$ , Equation [140] is then

$$\ln \left( \frac{\theta}{k} \sqrt{\frac{\rho U^2}{\tau_w}} \right) = \frac{1}{A} \sqrt{\frac{\rho U^2}{\tau_w}} - \frac{B_3}{A} - \frac{B_{2,R}}{A} + \ln D_1 - \frac{D_2}{D_1} \sqrt{\frac{\tau_w}{\rho U^2}} \quad [142]$$

If the term involving  $\sqrt{\frac{\tau_w}{\rho U^2}}$  is linearized with respect to  $\sqrt{\frac{\rho U^2}{\tau_w}}$  or

$$\sqrt{\frac{\tau_w}{\rho U^2}} = a_1 + a_2 \sqrt{\frac{\rho U^2}{\tau_w}} \quad [143]$$

then Equation [142] becomes in common logarithms

$$\log_{10} \left( \frac{\theta}{k} \sqrt{\frac{\rho U^2}{\tau_w}} \right) = O_1 \sqrt{\frac{\rho U^2}{\tau_w}} + P_1 \quad [144]$$

where

$$O_1 = \frac{1}{2.3026A} - \frac{a_2 D_2}{2.3026D_1} \quad [145]$$

and

$$P_1 = \frac{-B_3 - B_{2,R}}{2.3026A} - \frac{a_1 D_2}{2.3026D_1} + \log_{10} D_1 \quad [146]$$

Furthermore, if  $\log_{10} \sqrt{\frac{\tau_w}{\rho U^2}}$  is linearized with respect to  $\sqrt{\frac{\rho U^2}{\tau_w}}$  or

$$\log_{10} \sqrt{\frac{\tau_w}{\rho U^2}} = a_3 + a_4 \sqrt{\frac{\rho U^2}{\tau_w}} \quad [147]$$

Equation [144] becomes approximately

$$\log_{10} \frac{\theta}{k} = O_2 \sqrt{\frac{\rho U^2}{\tau_w}} + P_2 \quad [148]$$

or

$$\frac{\tau_w}{\rho U^2} = \frac{O_2^2}{\left(\log_{10} \frac{\theta}{k} - P_2\right)^2} \quad [149]$$

where

$$O_2 = O_1 + a_4 \quad [150]$$

and

$$P_2 = P_1 + a_3 \quad [151]$$

In the case of  $H$ , the substitution of Equation [148] into [141] produces

$$\frac{H}{H-1} = \left(\frac{D_1}{D_2} \frac{O_2}{O_1}\right) \log_{10} \frac{\theta}{k} - \frac{D_1 P_2}{D_2 O_2} \quad [152]$$

## QUASI-SMOOTH REGIME

In the case of the quasi-smooth regime  $B_1$  is constant,  $B_1 = B_{1,s}$ , and Equation [139] becomes

$$\ln R_\theta = \frac{1}{A} \sqrt{\frac{\rho U^2}{\tau_w}} - \frac{B_3}{A} - \frac{B_{1,s}}{A} + \ln D_1 - \frac{D_2}{D_1} \sqrt{\frac{\tau_w}{\rho U^2}} \quad [153]$$

If the term containing  $\sqrt{\frac{\tau_w}{\rho U^2}}$  is linearized with respect to  $\sqrt{\frac{\rho U^2}{\tau_w}}$  as in Equation [143],

Equation [153] is then in common logarithms

$$\log_{10} R_\theta = O_1 \sqrt{\frac{\rho U^2}{\tau_w}} + P_1' \quad [154]$$

or

$$\frac{\tau_w}{\rho U^2} = \frac{O_1^2}{(\log R_\theta - P_1')^2} \quad [155]$$

where  $O_1$  is given by Equation [145] and

$$P_1' = P_1 + \frac{B_{2,R} - B_{1,s}}{2.3026A} \quad [156]$$

An equation of the form of [155] was first derived by Squire and Young<sup>24</sup> for smooth surfaces.

The shape parameter  $H$  for quasi-smooth regime becomes after substituting Equation [154] into [141]

$$\frac{H}{H-1} = \left( \frac{D_1}{D_2 O_1} \right) \log_{10} R_\theta - \frac{D_1 P_1'}{D_2 O_1} \quad [157]$$

## ENGINEERING ROUGHNESS

In the case of engineering roughness,  $B_1$  is analytically defined as a function of  $k^*$  by Equation [110] which, since  $k^*$  is by definition

$$k^* \equiv \frac{R_\theta}{\theta/k} \sqrt{\frac{\tau_w}{\rho U^2}} \quad [158]$$

is written

$$B_1 = B_{1,s} - A \ln \left( 1 + \frac{R_\theta}{\lambda \theta/k} \sqrt{\frac{\tau_w}{\rho U^2}} \right) \quad [159]$$

For  $B_1$  given by Equation [159], Equation [139] becomes

$$-\ln \left( \frac{1}{R_\theta} + \frac{\sqrt{\frac{\tau_w}{\rho U^2}}}{\lambda \theta/k} \right) = \frac{1}{A} \sqrt{\frac{\rho U^2}{\tau_w}} - \frac{B_3}{A} - \frac{B_{1,s}}{A} + \ln D_1 - \frac{D_2}{D_1} \sqrt{\frac{\tau_w}{\rho U^2}} \quad [160]$$

If the term containing  $\sqrt{\frac{\tau_w}{\rho U^2}}$  is linearized with respect to  $\sqrt{\frac{\rho U^2}{\tau_w}}$  as in Equation [143],

Equation [160] is then in common logarithms

$$-\log_{10} \left( \frac{1}{R_\theta} + \frac{\sqrt{\frac{\tau_w}{\rho U^2}}}{\lambda \theta/k} \right) = O_1 \sqrt{\frac{\rho U^2}{\tau_w}} + P_1' \quad [161]$$

where  $O_1$  is given by Equation [145] and  $P_1'$  by [156].

Since no simple expression for  $H$  can be obtained from Equations [141] and [161], it

is necessary to retain  $\frac{\tau_w}{\rho U^2}$  as the intermediate parameter for calculating  $H$ .

## PREPARATION OF LOCAL SKIN FRICTION COEFFICIENT AND SHAPE PARAMETER DIAGRAMS FROM RESISTANCE CHARACTERIZATIONS

Where  $B_1$  is empirically stated as a function of  $k^*$  for any roughness configuration, a convenient method of preparing a diagram of  $\frac{\tau_w}{\rho U^2}$  and  $H$  plotted against  $R_\theta$  and  $\theta/k$  is by comparison with  $\frac{\tau_w}{\rho U^2}$  and  $H$  for the smooth case.

From Equation [139] for the same value of  $\frac{\tau_w}{\rho U^2}$  and in common logarithms

$$\log_{10} R_\theta - \log_{10} R_{\theta,s} = \frac{B_{1,s} - B_1}{2.3026 A} \quad [162]$$

Consequently, the resistance line of constant  $k^*$  or constant  $B_1$  for the rough case is offset from the smooth line by a constant amount in the direction of  $\log_{10} R_\theta$ .

To determine the resistance line of constant  $\theta/k$  from the lines of constant  $k^*$  the procedure is as follows:

Since by definition

$$R_\theta \equiv \frac{\theta}{k} \sqrt{\frac{\rho U^2}{\tau_w}} k^* \quad [163]$$

or

$$\log_{10} R_\theta = \log_{10} \theta/k - \log_{10} \sqrt{\frac{\tau_w}{\rho U^2}} + \log_{10} k^* \quad [164]$$

Hence for a given  $k^*$  and  $\theta/k$  the intersection of Equations [162] and [164] gives the desired point. A rapid way of plotting other lines of Equation [164] is to relate them to any

plotted line of [164] at constant  $\frac{\tau_w}{\rho U^2}$  or

$$\log_{10} R_{\theta,2} - \log_{10} R_{\theta,1} = \log_{10} (\theta/k)_2 - \log_{10} (\theta/k)_1 + \log_{10} k_2^* - \log_{10} k_1^* \quad [165]$$

The various plots of Equation [164] are then offset by constant amounts in the direction of  $\log_{10} R_\theta$ .

The procedure is the same for  $H$  since  $H$  is solely a function of  $\frac{\tau_w}{\rho U^2}$  from Equation [141].

## PREPARATION OF LOCAL SKIN FRICTION COEFFICIENT AND SHAPE PARAMETER DIAGRAMS FROM PLATE TESTS

To prepare diagrams of  $\frac{\tau_w}{\rho U^2}$  and  $H$  from total resistance results for an arbitrary roughness configuration, the following method may be employed:

From total resistance tests of a representative sample of a particular roughness the results are given in the form of  $C_f = f(R_x, x)$ . The objective of the analysis is to obtain

$\frac{\tau_w}{\rho U^2}, H = f(R_\theta, \theta)$ . From Equation [84] approximately

$$\frac{\tau_w}{\rho U^2} = \frac{C_f}{2} \left( 1 - 2A \sqrt{\frac{C_f}{2}} \right) \quad [166]$$

and from Equation [68]

$$R_\theta = \frac{1}{2} R_x C_f \quad [167]$$

and

$$\theta = \frac{1}{2} x C_f \quad [168]$$

To obtain lines of constant  $\theta$ , a line is first drawn at a fixed distance in the  $\log R_\theta$  direction from the smooth curve for each data point which corresponds to a line of constant  $k^*$  in accordance with Equation [162]. Then to locate the point corresponding to the desired value of  $\theta$  use is made of Equation [165] wherein for the same  $\frac{\tau_w}{\rho U^2}$ ,  $k^*$ , and  $k$

$$\log_{10} R_{\theta,2} - \log_{10} R_{\theta,1} = \log_{10} \theta_2 - \log_{10} \theta_1 \quad [169]$$

The reference line for using the above is from Equation [164]

$$\log_{10} R_\theta = -\log_{10} \sqrt{\frac{\tau_w}{\rho U^2}} + \text{constant} \quad [170]$$

the constant is any value convenient for plotting.

The values of  $H$  of the arbitrary roughness are calculated from Equation [141] wherein

$$H = \frac{1}{1 - \frac{D_2}{D_1} \sqrt{\frac{\tau_w}{\rho U^2}}} \quad [171]$$

The remainder of the procedure for determining  $H = f(R_\theta, \theta)$  is the same as that for  $\frac{\tau_w}{\rho U^2}$ .



## NUMERICAL RESULTS

The experimental difficulties in boundary-layer measurements have resulted in considerable discrepancies in numerical values of constants among investigators in the field.<sup>25</sup> Although future tests will thus in all probability lead to somewhat different values, the numerical results gathered and calculated by Landweber<sup>18</sup> have been judged to be as reliable as any and have been used to evaluate the factors derived in this report. For convenience of reference, the numerical values are listed in Table 3.

TABLE 3  
Numerical Values of Factors

Factor	Value	Source	Factor	Value	Source
$a_1$	0.0625	Calc.	$m$	1.076	Eq. [117]
$a_2$	$-7.57 \times 10^{-4}$	Calc.	$M_1$	0.242	Eq. [93]
$a_3$	-1.082	Calc.	$M_2$	0.262	Eq. [98]
$a_4$	$-1.306 \times 10^{-2}$	Calc.	$M_2'$	0.282	Eq. [106]
2.3026 $A$	6	Ref. 18	$N_1$	-0.661	Eq. [94]
$A$	2.6	Ref. 18	$N_1'$	0.023	Eq. [103]
$B_{1,s}$	4	Ref. 18	$N_2$	0.215	Eq. [99]
$B_{2,R}$	7.2	Fig. 10	$N_2'$	1.729	Eq. [107]
$B_3$	2	Ref. 18	$O_1$	0.1689	Eq. [145]
$C_1$	0.105	Calc.	$O_2$	0.1558	Eq. [150]
$C_2$	$-2.5 \times 10^{-3}$	Calc.	$P_1$	-1.169	Eq. [146]
$C_3$	-1.752	Calc.	$P_1'$	-0.636	Eq. [156]
$C_4$	-0.04	Calc.	$P_2$	-2.251	Eq. [151]
$D_1$	3.499	Ref. 18	$\nu$	24.66	Eq. [116]
$D_2$	23.23	Ref. 18	$\lambda$	3.42	Eq. [109]

Since the sand roughness values of Nikuradse<sup>†</sup> were obtained from pipe flow, some adjustment is needed for application to flat plates. The values of  $B_2$  of Nikuradse were obtained by using a value of 5.75 for 2.3026  $A$  which differs from the value of 6 used by Landweber for flat plates. Consequently the velocity profiles of Nikuradse were replotted and new  $B_2$  values for pipes were obtained using the slope of 6 as shown in Figure 10. The  $B_2$  values are converted to those for flat plates by assuming that the difference in such

<sup>†</sup>Here  $k$  refers to the size of the sand grains.

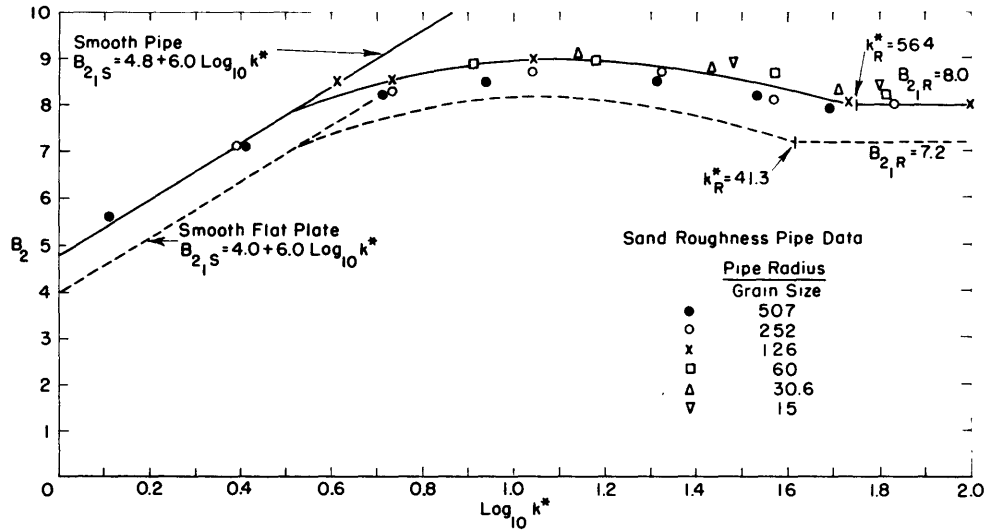


Figure 10 – Values of  $B_2$  for Sand Roughness in Pipes and on Flat Plates

values is equal to the difference in the  $B_{1,s}$  values between pipes and flat plates (here  $4.8 - 4.0 = 0.8$ ). For the fully rough regime, the  $B_{2,R}$  value of 8.0 for pipes becomes 7.2 for flat plates. In order to accommodate the new  $k_R^*$  values of 41.3 for flat plates, the  $k^*$  values are also adjusted for flat plates in the general rough regime. The procedure is to assume that the ratio of laminar sublayer thickness of flat plates to that of pipes for the quasi-smooth regime is the same for the general rough regime. From Equation [39]

$$r = \frac{y_L'^*}{y_L^*} = \frac{B_{1,s}' + A \ln A}{B_{1,s} + A \ln A} \quad [172]$$

where the primed quantities refer to flat-plate values and the unprimed quantities to pipe values. In terms of  $B_2$  values

$$r = \frac{B_2' + A \ln A - A \ln k'^*}{B_2 + A \ln A - A \ln k^*} \quad [173]$$

or

$$k'^* = (k^*)^r \exp \left[ \frac{B_2' - B_2}{A} + (1-r) \ln A \right] \exp \left[ \frac{(1-r) B_2}{A} \right] \quad [174]$$

The results which are given in Figure 10 were used to prepare the resistance diagram for sand roughness of Figure 7. Compared to the original Prandtl-Schlichting diagram,<sup>4</sup> the  $C_f$  values are somewhat lower for the same Reynolds number; this is to be expected considering that the Prandtl-Schlichting diagram is based on pipe results. Figure 11 gives a clearer indication of this where a comparison is made for the fully rough regime.

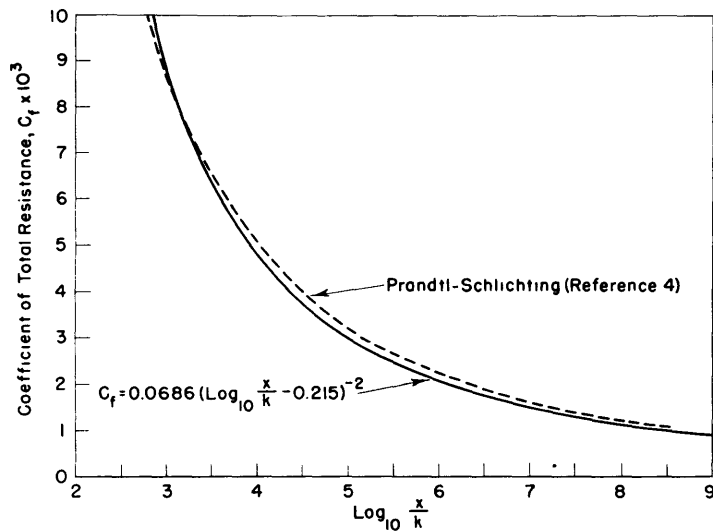


Figure 11 – Coefficients of Total Resistance for the Fully Rough Regime

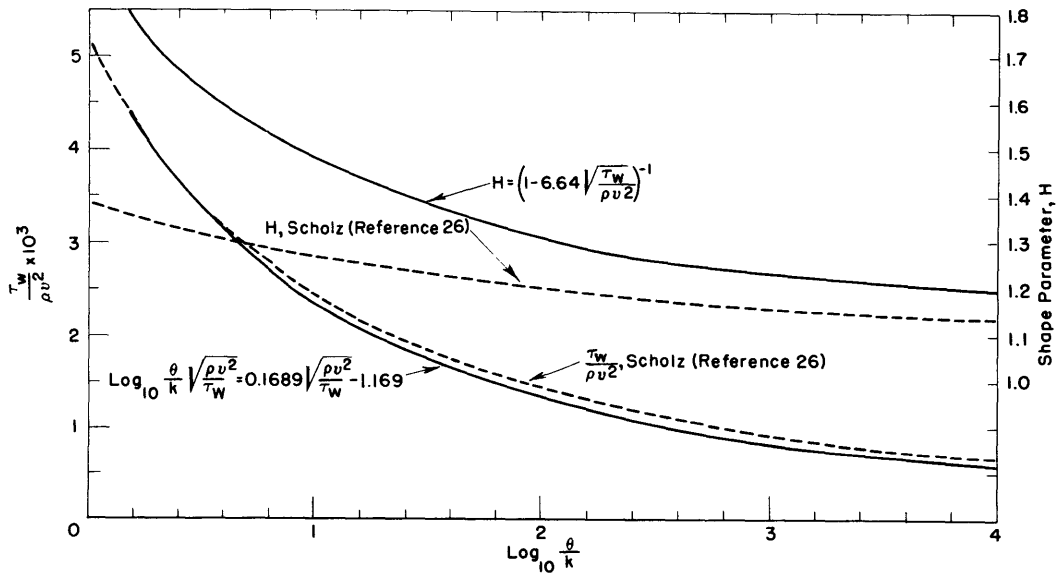


Figure 12 – Local Skin Friction and Shape Parameter for the Fully Rough Regime of Flat Plates

For the total resistance of smooth plates, the new  $M_1$  value of 0.242 is identical to that of the Schoenherr formula and the new  $N_1'$  value of 0.023 is close to that of zero for the Schoenherr formula.

Finally, for the fully rough regime Figure 12 shows a comparison of local resistance coefficients and  $H$  values from Equations [144] and [141] to those of Scholz<sup>26</sup> obtained by a simple power-law analysis of the Prandtl-Schlichting formula. The local resistance coefficients compare well but the  $H$  values show a large difference which is due to the improper power-law analysis of Scholz.

## ACKNOWLEDGMENT

The author wishes to express his appreciation to Mr. Ralph D. Cooper for his critical review of this report.

## REFERENCES

1. Prandtl, L., "The Mechanics of Viscous Flows," Vol. III of "Aerodynamic Theory," W.F. Durand, ed., Julius Springer, Berlin (1935).
2. Von Kármán, T., "Mechanical Similitude and Turbulence," NACA TM 611 (Mar 1931), (Translation from Nachr. Ges. Wiss. Göttingen, 1930).
3. Von Kármán, T., "Skin Friction and Turbulence," Journal of the Aeronautical Sciences, Vol. 1, No. 1 (Jan 1934).
4. Prandtl, L. and Schlichting, H., "The Resistance Law for Rough Plates," David Taylor Model Basin Translation 258 (Sep 1955), (translation from Werft-Reederei-Hafen, Jan 1934).
5. Nikuradse, J., "Laws of Flow in Rough Pipes," NACA TM 1291 (Nov 1950), (translation from VDI - Forsch. 361, 1933).
6. Squire, H.B., "Reconsideration of the Theory of Free Turbulence," Philosophical Magazine, 7th Series, Vol. 36, No. 288 (Jan 1948).
7. Laufer, J., "Investigation of Turbulent Flow in a Two-Dimensional Channel," NACA TN 2123 (July 1950) or NACA Report 1053 (1951).
8. Batchelor, G.K., "Note on Free Turbulent Flows, with Special Reference to the Two-Dimensional Wake," Journal of the Aeronautical Sciences, Vol. 17, No. 7 (Jul 1950).
9. Schubauer, G.B., "Turbulent Processes as Observed in Boundary Layer and Pipe," Journal of Applied Physics, Vol. 25, No. 2 (Feb 1954).
10. Clauser, F.H., "Turbulent Boundary Layers in Adverse Pressure Gradients," Journal of the Aeronautical Sciences, Vol. 21, No. 2 (Feb 1954).
11. Millikan, C.B., "A Critical Discussion of Turbulent Flows in Channels and Circular Tubes," Proceedings of the Fifth International Congress for Applied Mechanics, Cambridge, Mass. (1938), John Wiley and Sons, New York (1939).
12. Rotta, J., "Das in Wandnähe gültige Geschwindigkeitsgesetz turbulenter Strömungen," (The Velocity Law Which Is Valid in the Vicinity of the Wall for Turbulent Flows), Ingenieur-Archiv, Vol. 18, No. 4 (1950).
13. Hudimoto, B., "A Brief Note on the Laminar Sub-Layer of the Turbulent Boundary Layer," Memoirs of the Faculty of Engineering, Kyoto Univ. (Japan), Vol. 13, No. 4 (Oct 1951).

14. Hama, F.R., "On the Velocity Distribution in the Laminar Sublayer and Transition Region in Turbulent Shear Flows," *Journal of the Aeronautical Sciences*, Vol. 20, No. 9 (Sep 1953).
15. Van Driest, E.R., "On Turbulent Flow Near a Wall," North American Aviation Report AL - 2077 (Oct 1954); also, 1955 Heat Transfer and Fluid Mechanics Institute at Univ. of Calif., Los Angeles; also, *Journal of the Aeronautical Sciences*, Vol. 23, No. 11 (Nov 1956).
16. Laufer, J., "The Structure of Turbulence in Fully Developed Pipe Flow," NACA TN 2954 (Jun 1953).
17. Goldstein, S., "A Note on Roughness," (British) Aeronautical Research Committee R & M 1763 (Jul 1936), Vol. 51 (1937).
18. Landweber, L., "The Frictional Resistance of Flat Plates in Zero Pressure Gradient," *Transactions of the Society of Naval Architects and Marine Engineers*, Vol. 61 (1953); also, "Der Reibungswiderstand der Längsangeströmtenebene Platte," *Jahrbuch der Schiffbautechnischen Gesellschaft*, Vol. 46 (1952).
19. Colebrook, C.F., "Turbulent Flow in Pipes, with Particular Reference to the Transition Region between the Smooth and Rough Pipe Laws," *Journal of the Institution of Civil Engineers*, Vol. 11 (1938/39).
20. Granville, P.S., "The Viscous Resistance of Surface Vessels and the Skin Friction of Flat Plates," *Transactions of the Society of Naval Architects and Marine Engineers*, Vol. 64 (1956).
21. Couch, R.B., "Preliminary Report of Friction Plane Resistance Tests of Anti-Fouling Ship Bottom Paints," David Taylor Model Basin Report 789 (Aug 1951).
22. Granville, P.S., "A Method for the Calculation of the Turbulent Boundary Layer in a Pressure Gradient," David Taylor Model Basin Report 752 (May 1951).
23. Granville, P.S., "The Calculation of the Viscous Drag of Bodies of Revolution," David Taylor Model Basin Report 849 (Jul 1953).
24. Squire, H.B. and Young, A.D., "The Calculation of the Profile Drag of Aerofoils," (British) Aeronautical Research Committee R & M 1838 (Nov 1937).
25. Hama, F.R., "Boundary-Layer Characteristics for Smooth and Rough Surfaces," *Transactions of the Society of Naval Architects and Marine Engineers*, Vol. 62 (1954).
26. Scholz, N. "Über eine rationelle Berechnung des Strömungswiderstandes schlanker Körper mit beliebig rauher Oberfläche," (On a Rational Calculation of the Flow Resistance of Slender Bodies with Arbitrarily Rough Surfaces), *Jahrbuch der Schiffbautechnischen Gesellschaft*, Vol. 45 (1951).



# INITIAL DISTRIBUTION

Copies	Copies	Copies
<p>17 CHBUSHIPS, Library (Code 312)  5 Tech Library  1 Tech Asst to Chief (Code 106)  2 Appl Sci (Code 370)  2 Design (Code 410)  3 Prelim Design (Code 420)  1 Dr. S. Silverstein  3 Submarines (Code 525)  1 Propellers &amp; Shafting (Code 554)</p> <p>5 CHBIFORD, Underwater Ord (Re5a)  1 Dr. A. Miller  1 Mr. M.A. Egeers</p> <p>3 CHBIAER  2 Aero &amp; Hydro Br (DE-3)  1 Appl Math Br</p> <p>4 CHOHK  1 Mathematics (Code 432)  2 Mechanics (Code 438)  1 Undersea Warfare (Code 466)</p> <p>2 Dir, USNRL</p> <p>4 CDR, USNOL, Tech Div</p> <p>2 CDR, USNOTS, China Lake, Calif.  1 Underwater Ord Div, Pasadena Annex</p> <p>1 NAVSHIPYD HAPC</p> <p>1 NAVSHIPYD HORVA</p> <p>2 NAVSHIPYD PTCSH  1 Capt L.A. Rupp</p> <p>1 CDR, USNPG, Dahlgren, Va.</p> <p>1 CDR P DIP, USNUSL, New London, Conn.</p> <p>2 CO, USNUSOS, Design Section, Newport, R.I.</p> <p>1 CO, USNATC, Patuxent River, Md.</p> <p>1 Supt, USN Postgrad Sch, Monterey, Calif.</p> <p>1 Dir, Marine Physical Lab, USNHEL, San Diego, Calif.</p> <p>1 Chrm, Defense Science Board</p> <p>1 Dir, Aero Res Lab, Wright Air Dev Ctr  Wright-Patterson AFB, O.</p> <p>1 Tech Info Div, Library of Congress</p> <p>2 Chief, ASTIA Document Ctr, Arlington, Va.</p> <p>1 Dir, Ballistic Res Lab, Aberdeen Proving Ground,  Aberdeen, Md.</p> <p>2 Dir of Res, Engr Res &amp; Dev, Fort Belvoir, Va.</p> <p>1 Dir, Tech Info Gr, Aberdeen Proving Ground,  Aberdeen, Md.</p> <p>1 Dir, NACA</p> <p>3 Dir, Langley Aero Lab, Langley AFB, Va.  1 Dr. A.F. von Doenhoff  1 Mr. H. Teteriva</p> <p>2 Dir, Lewis Fl Propul Lab, Cleveland, O.</p>	<p>2 Dir, Ames Aero Lab, Moffett Field, Calif.</p> <p>1 Dir, Oak Ridge Yatt Lab, Oak Ridge, Tenn.</p> <p>2 Chief, Natl Hydr Lab, Natl BuStands</p> <p>2 Hydro Lab, Altn Exec Com, CIT, Pasadena, Calif.</p> <p>1 Dir, Inst of Engr Res, Univ of Calif, Berkeley, Calif.</p> <p>2 Colorado State Univ, Dir, Hydr Lab, Ft. Collins, Colo.  1 Mr. B. Chanda, Dept of Civ Engr</p> <p>2 Dir, Iowa Inst of Hydr Res, State Univ of Iowa, Iowa City,  Ia.  1 Dr. L. Landweber</p> <p>3 Dir, Inst for Fluid Dynamics &amp; Appl Math, Univ of Maryland  College Park, Md.  1 Prof. J.P. Beske  1 Dr. F.R. Hama</p> <p>2 Dir, Exper Nav Tank, Dept NAME, Univ of Michigan,  Ann Arbor, Mich.</p> <p>2 Dir, ETT, SIT, Hoboken, N.J.  1 Dr. J.P. Breslin</p> <p>1 Dir, Jet Propul Lab, CIT, Pasadena, Calif.</p> <p>1 Dir, Defense Res Lab, Univ of Texas, Austin, Tex.</p> <p>1 Dir, St Anthony Falls Hydr Lab, Univ of Minnesota,  Minneapolis, Minn.</p> <p>2 Dir, ORL, Penn State Univ, University Park, Pa.</p> <p>1 Dir, Midwest Res Inst, Kansas City, Mo.</p> <p>1 Dir, Robinson Model Basin, Webb Inst of Nav Arch,  Glen Cove, L.I., N.Y.</p> <p>2 Head, Dept NAME, MIT, Cambridge, Mass.  1 Prof. Abkowitz</p> <p>2 SHIPSHIP'SORD, General Dynamics Corp, Groton, Conn.  1 Electric Boat Division</p> <p>2 NISB P DDCo, Newport News, Va.  1 Sr Naval Architect  1 Sup, Hydr Lab</p> <p>1 Editor, Aero Engr Review, New York, N.Y.</p> <p>1 Editor, Appl Mech Review, Southwest Res Inst,  San Antonio, Tex.</p> <p>1 Editor, Bibliography of Tech Reports, Office of Tech Serv  U.S. Dept of Commerce</p> <p>1 Editor, Engr Index, New York, N.Y.</p> <p>1 Editor, Mathematical Reviews, Brown Univ, Providence, R.I.</p> <p>2 Tech Library, Douglas Aircraft Co., Inc., El Segundo, Calif.  1 Mr. A.H.O. Smith</p> <p>2 Tech Library, North Amer Aviation, Inc., Downey, Calif.  1 Dr. E.R. van Driest</p> <p>2 Dir, Aero Res Lab, Melbourne, Australia</p>	<p>1 Dir, Inst of Aerophysics, Univ of Toronto, Toronto, Canada</p> <p>3 NPL, Teddington, England  1 Aero Div  2 Ship Div</p> <p>1 Head, Aero Dept, Royal Aircraft Estab,  Farnborough, Hants, England</p> <p>1 Dr. S.L. Smith, Dir, BSHA, London, England  1 H. Lackenby</p> <p>1 Dir, Bassin d'Essais des Calénes 6, Paris, France</p> <p>1 Dir, Societe Grenblose d'Etudes et d'Applications  Hydrauliques, Grenoble, (Isère) France</p> <p>1 Office, Natl d'Etudes et de Recherches Aéronautique 3,  Paris, France</p> <p>1 Dr. J. Druodonné, Dir, Institut de Recherches de la  Construction Navale, Paris, France</p> <p>2 O.N.E.R.A., Service des Relations Extérieures et de la  Documentation, Châtillon-sous-Bagneux (Seine), France</p> <p>1 Prof. Dr. H. Schlichting, Institut für Stömungs, Technische  Hochschule, Braunschweig, Germany</p> <p>1 Gen. Ing. u. Pugliese, Pres., Instituto Naz. per Studi ed  Esp. di Arch Nav, Rome, Italy</p> <p>1 Dir, Laboratorium Voor Aero-En Hydrodynamica, Delft,  Netherlands</p> <p>1 Dr. F. Lopez Acevedo, Dir, Canal de Experiencias Hidrodina-  micas, Madrid, Spain</p> <p>1 Dir, Nederland Scheepsbouwkundig Proefstaben, Wageningen,  Holland</p> <p>1 Dr. Hans Edstrand, Dir, Statens Skeppsprovvningsanstalt,  Goteborg, Sweden</p> <p>1 Dir, Library of Chalmers Univ of Tech, Goteborg, Sweden</p> <p>2 Dir, Institut für Schiffbau der Universität Hamburg,  Hamburg, Germany  1 Dr. K. Weghardt</p> <p>1 Dr. H.W. Lerbs, Hamburgische Schiffbau-Versuchsanstalt,  Hamburg, Germany</p> <p>1 Dir, ARL, Teddington, England</p>









MIT LIBRARIES

DUPL



3 9080 02754 2171

